INVESTIGATION OF THE LASING MECHANISM OF AN HCN MOLECULAR LASER

Thesis submitted for the Degree of
Doctor of Philosophy [M.Phil. awarded]
in the
University of Southampton
by

R. H. Khan

Department of Electronics
University of Southampton

March 1970

SUMMARY

This thesis describes the construction and operation of various HCN laser systems with a view to determine the mechanism of operation.

In one system to simplify the processes occuring within the discharge tube, nitrogen was excited by a microwave discharge before entering the cavity. This coupled with the thermal decomposition of a peroxide reduced the d.c. threshold current for laser operation down to 5mA. CW laser oscillation in pure HCN was studied together with the influence of foreign gases on the laser.

It is concluded that a simple one or two stage process does not produce the population inversion but that a multiple stage process, which could be difficult to identify, is always involved.

CONTENTS

CHAPTER 1 INTRODUCTION

Nitrogen was the first molecular gas in which laser oscillations were produced. Using a pulsed electrical discharge, Mathias and Parker (Ref.1) detected oscillations on 28 wavelengths, in the near infra-red region, and identified them as electronic transitions belonging to the band spectrum of the nitrogen molecule. Using the same experimental arrangement Mathias and Parker (Ref. 2) also obtained laser oscillations, at numerous wavelengths in the visible region, from carbon monoxide. The lasing transitions were again identified as belonging to the band system of the molecule. These early experiments suggested that, in principle, population inversion could be achieved on a vibrational or rotational transition in a molecule. Due to the smaller energy gaps involved, a laser oscillating on a vibrational transition would have a wavelength lying in the near or medium infra-red, whereas a pure rotational laser would oscillate in the far infra-red region.

The first far infra-red laser reported (Ref. 3) used water vapour as the active medium. Since then oscillations, on over a 100 lines in the far infra-red, have been obtained in a considerable number of molecules, the longest wavelength being 774μm in a discharge through ICN (Ref. 4). A strong line at 337μm was first observed by Gebbie et al. (Ref. 5), in a pulsed

fields, these shifts could be of the order of 10^4 times the Doppler width of the line.

The frequencies of many submillimetre lasers have been directly measured (e.g. Ref. 21, 22). This, coupled with an accurate measurement of the wavelength of the transition, presents a possibility for the direct determination of the velocity of light. The accuracy quoted for the frequency measurements is about 1 part in 10^6 but with frequency stabilization this should be easily improved by a few orders of magnitude. Thomas (Ref. 55) has proposed a scheme for accurately measuring the wavelength of such a stabilized submillimetre laser by comparing it with the wavelength of a He-Ne laser. The He-Ne laser is stabilized on the Lamb-dip and this laser, in turn, is absolutely calibrated by comparison with the standard ^{86}Kr line in a Fabry-Perot interferometer. The overall accuracy in determining the wavelength of the submillimetre laser would thus be almost 1 part in 10^8 (the Lamb-dip stabilized laser having a long term stability of 1 in 10^8). As the accuracy of the frequency measurement is better than this, the velocity of light can then be determined to this accuracy, i.e. about 1 part in 10^8. Daneu et al. (Ref. 56) have performed an experiment on these lines, using H_2O and D_2O submillimetre lasers, and from a preliminary measurement the velocity of light was determined to 1 part in 10^6. This is

nearly the accuracy of the present accepted value of the velocity of light. The accuracy can be easily improved by proper stabilization of the submillimetre laser and better facilities for counting the fringes in the interferometer. Stabilized submillimetre lasers, when developed with long term stabilities, could serve as wavelength standards in the far infra-red. Such standards are needed in the far infra-red and these lasers could be periodically calibrated absolutely by a standard krypton line.

One of the uses of an HCN laser would be to measure the electron densities in plasmas. As the phase shift of light passing through a plasma is proportional to its wavelength, submillimetre lasers are ideally suited for this purpose. For example, in comparison with a He-Ne laser operating at 3.39μm, the HCN laser at 337μm would be a factor of 100 more sensitive. Using appropriate focussing arrangements, Kon et al. (Ref.52) were able to make spatially resolved measurements on a high density helium plasma. The minimum density detectable with the system was $8 \times 10^{12}/d$ cm^{-3}, where d is the length of the plasma in centimetres.

The aim of this project was to determine the origin of the 337μm, and other associated, laser lines. There was no information on what species was responsible. Theories assigning the CN radical as the lasing species did not seem to be valid. An experimental technique, previously applied to He-Ne lasers (Ref. 41) was proposed to determine the mechanism of the laser. The

technique depends on the fluctuation of the spontaneous emission, from levels associated with the laser transition, when the resonant cavity is modulated. This is described in section 4.2, and a scan of the spontaneous emission over the range 0.2 to 22μm was to be attempted. Lide and Maki (Ref. 28), at this stage, proposed a scheme for the laser involving vibrational states of the HCN molecule in the ground electronic state. The application of the proposed technique to verify the assignment by Lide and Maki, was roughly calculated as being not feasible. However, there is an excellent agreement between the observed and calculated frequencies for the laser transitions and, in addition, most of the observed properties of the laser can be explained in terms of the HCN model.

Although the lasing levels were identified, there was no explanation of the mechanism of inversion of the levels. As the laser operates with a variety of compounds, HCN must at some stage be chemically formed in the discharge. For the inversion, Lide and Maki postulated that the HCN is formed in the discharge preferentially with a quanta of the C-H stretching mode of vibration. This leads to an inverted population between the $11^{1}0$ and $04^{0}0$ states of the molecule. In the project, attempts were made to determine whether the HCN is formed in the discharge with an inverted population or whether the HCN, formed in the

ground state, has to be excited by some other means. It is known that active nitrogen (the name given to nitrogen subjected to an electrical discharge) reacts with a variety of hydrocarbons to produce HCN as the primary product and sections 4.3 and 4.4 describe the experiments in which the laser was operated with a mixture of hydrocarbons and active nitrogen. In mixtures containing nitrogen, for example CH_4-N_2, the threshold current for laser operation was found to be significantly lowered when the nitrogen was subjected to an electrical discharge before entering the laser cavity. It is however shown that no d.c. discharge should have been necessary if this was the only mechanism involved. Section 4.5 describes attempts to obtain laser action by chemically combining active nitrogen and methyl radicals. This again was not successful but in an experiment where a peroxide was thermally decomposed to provide methyl radicals, a laser threshold current of only 4mA was obtained. This is roughly a factor of 30 lower than the threshold for normal d.c. operation. In order to separate the processes of the formation and inversion of the HCN molecule, experiments were then performed using pure HCN. It was seen that under no condition does HCN perform as well as some organic mixtures. The laser output is lower and the rate of decomposition of the polymer on the tube walls is extremely rapid.

In the conclusions it is shown that the mechanism of inversion of the HCN molecule cannot be a simple single stage process but that numerous processes are involved. For example, starting with a methane-nitrogen mixture, the processes could be:

1. Nitrogen dissociates partially into N atoms.
2. The hydrogen atoms of the methane are stripped by the action of the discharge and CH_3, CH_2 and CH radicals are present.
3. Methane as well as the radicals produced could combine with the N atoms present to give HCN.
4. Intermediate species are formed with vibrational excitation. With the number of reactive species present, the combinations possible are numerous. Consequently the possibility of more than one species having an appropriate vibrational energy (for transfer to HCN) is high considering the large energy defect allowable for this process.
5. There is a vibrational energy transfer from the intermediate species to HCN resulting in an inversion.

CHAPTER 2 REVIEW OF THE HCN LASER

2.1 Introduction to the HCN Laser

Using hydrogen cyanide in a 9.3 metre long discharge tube, Gebbie et al.(Ref.5) first obtained the 337μm laser line. The wavelength was measured to an accuracy of ± 1μm, and within these limits, the same wavelength was observed in discharges through methyl cyanide and ethyl cyanide. Pulses of approximately 1μsec duration were used and it was noted that, with a static filling of the gas, oscillations could only be maintained for a few hundred pulses. Almost all subsequent workers have used systems with a continuous gas flow.

The 337μm line, as well as ten additional lines ranging from 126 to 373μm, were observed by Mathias et al.(Ref.6) in a pulsed discharge through dimethylamine. Many of these lines were also observed in discharges through a variety of compounds containing hydrogen, carbon and nitrogen. To give an idea of the number of compounds used, oscillations were obtained with monomethylamine, trimethylamine, diethylamine, ethylene-diamine, ethyleneimine, pyridine, methyl cyanide, and with mixtures of hydrogen and bromine cyanide, methane and bromine cyanide, ammonia and bromine cyanide, and methane and ammonia. If deuterium was substituted for hydrogen in any of these compounds, lasing action was

obtained, but with a completely different spectrum. The wavelengths and peak output powers obtained with dimethylamine are given in Table 1. The four stronger lines (marked 'a') are also observed with many other compounds and mixtures containing hydrogen, carbon and nitrogen. The table also gives the wavelengths of the lines obtained if deuterium is substituted for hydrogen - a mixture of deuterium and bromine cyanide being used as the active material.

Continuous operation on the two intense lines at 311 and 337μm was obtained by Muller and Flescher (Ref.7) in methyl cyanide with a 1.2amps d.c. current through the discharge. They also obtained the same lines using mixtures of either acetone or benzene with nitrogen. Encountering the problem of polymer deposition on the walls of the discharge tube, they found that running a discharge through water vapour slowly cleans the deposit. During this cleaning operation, oscillations on the 311 and 337μm lines were obtained. Following this a mixture of methyl cyanide and water vapour was used giving strong oscillations, on the 311 and 337μm lines, with the rate of contamination greatly reduced. The partial pressures of the methyl cyanide and water vapour were in the ratio of 1:10.

The thick brown polymer which is deposited on the walls of the laser tube during operation causes, eventually, a decrease in

Table 1

Values taken from Ref.6

Laser Wavelengths from a Pulsed Discharge through Dimethylamine

Wavelength (μm)	Approximate Peak Power (W)
126.24	1
128.75[a]	1
130.95[a]	1
135.03	0.2
201.19	0.005
211.14	0.04
223.25	0.003
309.94	0.4
311.08[a]	0.7
336.83[a]	7
372.80	0.1

(Lines marked 'a' have been observed with many compounds containing H, C and N.)

Laser Wavelengths from a Pulsed Discharge through a Mixture of Deuterium and Bromine Cyanide

Wavelength (μm)	Approximate Peak Power (W)
181.90	0.1
190.08	0.1
194.83	0.02
204.53	0.04

the output power of the laser. Hence, as the output powers from different organic solutions do not vary considerably, one of the criterion for choosing the lasing material seems to be that of minimum polymer formation. A mixture of methane and nitrogen gives a relatively clean discharge (Ref.11), and is now widely used.

Similar work on the HCN laser has been done by many independent workers using a wide range of compounds containing carbon, hydrogen, and nitrogen (Ref. 8-13). There has been only one report of a laser emission at 12.83μm in a mixture of methane and nitrogen (Ref.24).

The highest output power at 337μm has been reported by Kotthaus (Ref.16) in a continuously flowing mixture of ether vapour and nitrogen. Using a coupling hole of about 25mm diameter, at the end of a 6.5 metre long and 10cm diameter discharge tube, a laser output of 600mW was obtained. The d.c. current through the discharge tube was 1.2amp. The output power from the laser was plotted against the diameter of the coupling hole, and it was found that the laser could oscillate with a coupling hole diameter as large as 60mm. The optimum diameter of the coupling hole, 25mm, could account for the lower powers that have been reported by other workers. For example, the 24mW/metre power obtained by Stafsudd and Yeh (Ref.15) was

through a coupling hole of only a 3mm diameter. Again, in many cases, since oscillations were also required on other lines which do not have as high a gain as the 337μm transition, large output coupling holes could not be used.

2.2 Time Dependence of the Output Power of the HCN Laser

To gain an insight into the inversion mechanism, several workers have studied the time dependence of the power output of the HCN laser. In a pulsed HCN laser, Sochor and Brannen (Ref.17) found that the laser pulse occured 6 to 8μsec after the end of the current pulse. This behaviour was repeatable for current pulse lengths varying from 2 to 20μsec. These results were also obtained by Yamanaka et al. (Ref.18). They used a system with a static gas filling and this has to be taken into account when comparing their results with those of other workers. From their data it can be deduced that the pulse length increases linearly from about 20 to 120μsec, with the number of discharge pulses through the gas, and then rapidly decreases. A pulse repetition frequency of about 10Hz was used and the peak output power from the laser occured after about 110 current pulses.

In the same system, for certain lengths of the current pulse, multiple laser output pulses were observed. Up to three separate laser pulses were recorded with peaks roughly 10μsec apart. The interval between the peaks was seen to increase as the pressure

in the discharge tube was decreased. This effect has been observed more clearly by Turner et al. (Ref.19) using pulses of higher current through the discharge. The addition of various other gases to the lasing mixture was studied and they were seen to have a significant effect on the behaviour of the laser output. For example, helium increased the number of laser output pulses, their amplitude, and also the time during which they were emitted. The pressure of the mixture of methyl cyanide and helium could be adjusted to produce six laser pulses, approximately 90μsec apart, during a 450μsec period.

A longer delay between the current pulse and the laser output has been reported by Jones et al. (Ref.20). They observed a similar multiple pulse behaviour of the laser output, but the emission of the first pulse did not occur until 750μsec after the discharge pulse. Two factors could account for the difference between their observations and those due to Turner et al. First, the current density used by Jones et al. was a factor of about 25 lower than that used by Turner et al., and secondly the difference in lasing materials - propylamine being used by the former and methyl cyanide by the latter.

Schawlow (Ref.47) has studied the interaction of the electrons of the plasma with the laser radiation within the cavity and, in terms of this, most of the observations referred to above can be explained. Radiation at 337μm would be expected

to have a much stronger interaction with the electrons than radiation at optical wavelengths. For the case of the HCN laser plasma, this interaction was found to take the form of refraction. By diffusion theory, the radial distribution of the electrons in the discharge tube can be obtained and this distribution constitutes a divergent refracting element. The extent of the divergence is determined by the electron density and hence, for sufficiently high densities, the resonator becomes unstable. In a n-propylamine discharge, peak electron densities ranging from 10^{14}-2.2 x 10^{14}/cc were measured for 4μsec pulses of 1-5K amps peak currents, and it could be shown that this magnitude of the density was sufficient to strongly affect laser operation. A rough calculation shows the change in refractive index for an electron density of 10^{14}/cc to be 0.5%. The delay between the current and laser pulses can thus be associated with the decay time of the electrons (by diffusion and recombination with ions) to provide a stable cavity for oscillation. This could explain the time behaviour of the laser output observed by Sochor and Brannen (Ref.17). Also, a dependence of the delay time on cavity length has been observed by some workers (Ref. 20 and 48). Increasing the cavity length from the resonant position decreases the delay for laser emission and vice versa. This behaviour could be expected for lower electron densities where the divergence effect is very small, and an increase of the cavity

length compensating, to some extent, the change in refractive index of the plasma.

The multiple pulse emission observed with higher pulse currents (Ref. 18-20) can be explained by the presence of resonator modes which seem to include reflections from the walls of the tube. The higher electron densities resulting from the higher currents create divergent elements of larger values. The electron density takes a relatively longer time to reach a stable resonator condition, and during this interval multiple pulses are emitted due to modes which were proved to depend on reflections from the walls. Placing absorbing elements along the walls of the discharge tube completely suppressed the multiple pulses. Also, unstable resonators with convex elements could be made to oscillate only when no absorbers were placed along the walls. The presence of helium in the discharge tube would also slow the decay of the electrons and longer time intervals between the laser pulses could be expected. This was the effect observed by Turner et al. (Ref.19).

2.3 Absolute Frequency Measurements of the HCN Laser Transitions

Accurate measurements of the wavelengths in the far infra-red are very difficult. Hocker et al. (Ref.21) solved the problem of obtaining accurate spectroscopic information on the HCN laser transitions by measuring their frequency. They quote an accuracy of a few parts in 10^7 for the frequency measurements of the

311 and 337μm lines. The technique employed was beating the laser output with the 12th and 13th harmonics, for the 311 and 337μm lines respectively, of a V-band klystron operating near 85GHz. The laser was coupled through a horn into the input waveguide of a cross-guide harmonic crystal mixer which detected the beat notes.

In a later series of experiments, using a considerably larger laser, Hocker and Javan (Ref.22) measured the frequency of three additional HCN laser lines at 310, 335 and 373μm. These three transitions are weak compared to the 311 and 337μm lines, and this was the first report of their continuous operation. As can be seen from Fig.1, these lines are cascade transitions coupled to the 311 and 337μm transitions. The 310 and 373μm lines, for example, will only be obtained when the 337μm line is oscillating strongly.

2.4 Gain Measurements on the HCN Laser

Gain measurements on a pulsed HCN laser were made by Kon et al. (Ref.9) using the maximal loss method (Ref.31). A gain of 30% per metre was obtained for the 337μm transition. This value of the gain is considerably lower than the 70% per metre value reported by Jones et al. (Ref.20). The main factor responsible for this discrepancy is probably the use of a static gas filling by the former workers whereas the system used by

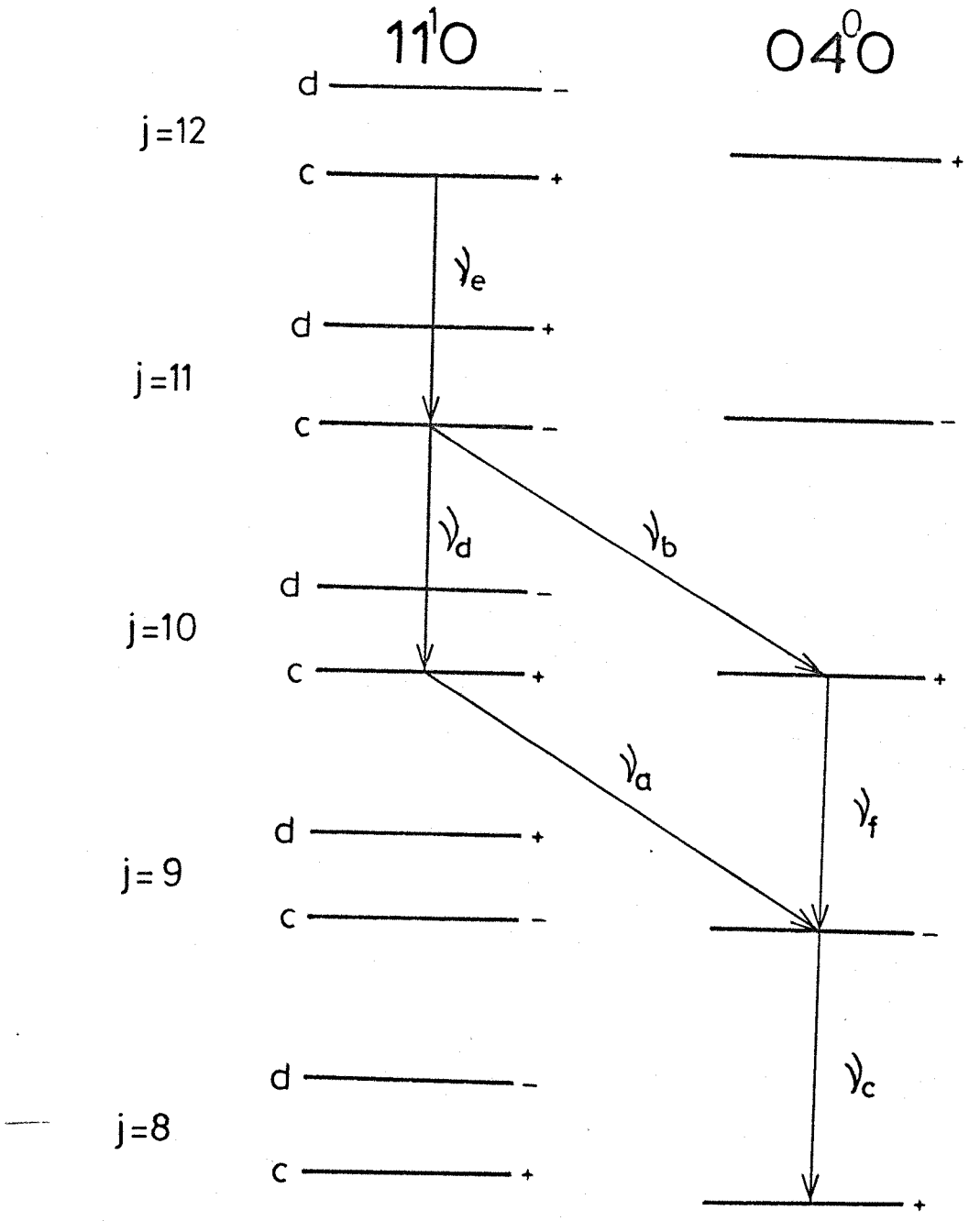
$11^{1}0$
$04^{0}0$
d
c
j=12
j=11
j=10
j=9
j=8
γ_e
γ_d
γ_b
γ_a
γ_f
γ_c

FIG 1

Jones et al. employed a continuously flowing gas mixture. Also, instead of the maximal loss method, Jones et al. measured the gain by passing the output of a continuous HCN laser through a pulsed discharge in propylamine vapour and noting the enhancement. To eliminate errors from changes in discharge conditions, the pulsed discharge was optimized for laser operation immediately prior to a gain measurement.

Using a technique similar to the one described above, Jones et al. (Ref.20) also measured the gain of a CW HCN laser by passing the output from a pulsed laser through a continuous discharge. A gain of 10% per metre was obtained. Kotthaus (Ref.16) has worked out the value of the gain as 20% per metre. This comparatively high value of the gain is probably accounted for by the assumptions made by Kotthaus in his calculations. Kotthaus has used the expressions derived by Boyd and Gordon (Ref.32) for the modes of a confocal resonator with rectangular mirrors to estimate the intensity of the TEM_{oo} mode being transmitted through an aperture in the output mirror at threshold, i.e. when about 90% of the intensity was estimated as being coupled out. This step is not valid because under the conditions when large coupling holes are introduced into a cavity, the modes are significantly perturbed and, in general, the TEM_{oo} mode is not necessarily the one with the lowest loss per pass. This means that, as the coupling hole is increased to a size where the

laser is oscillating just above threshold, the oscillations are generally on a higher order mode of the cavity. Work on these lines has been done by McCumber (Ref.30) but the data does not extend to such large couplings.

Also the assumption, that the flat-spherical mirror configuration used in the experiment is equivalent to a spherical-spherical configuration, is not justified. Kotthaus refers to the observations made by Turner et al. (Ref.19) in which there was no significant change in the laser output when different mirror configurations, for example confocal, flat-spherical etc., were used. However, the importance of the Fresnel number of the mirrors ($= \frac{a^2}{d\lambda}$, where a is the radius of the mirrors, d the distance between them, and λ the wavelength) seems to have been overlooked. In the resonant cavity used by Turner et al., with mirrors of Fresnel number 8.54, the curves plotted by Li (Ref.29) indicate losses of less than 0.1% per pass for confocal and folded resonators and about 1% for a plane-parallel resonator. This implies, as was observed by Turner, that different mirror configurations would not have an appreciable effect on the output power. This would not be the case in the cavity used by Kotthaus as the Fresnel number of the mirrors is only 1.14, and from the curves of Ref.29 the losses would vary from less than 0.1% to about 15% per pass between the confocal and plane-parallel cases. For the actual mirror configuration used in the experiment, the loss per pass is about 6%. Consequently, the assumption of

neglecting diffraction losses appears to be inaccurate.

Corcoran et al. (Ref.14) have published curves for the unsaturated gain characteristics of the 337μm transition against current for various mixtures of methyl cyanide and water vapour. In the experiment the output from a continuous laser operating at 337μm was passed through an amplifier cell, and the enhancement of the radiation passing through was used to calculate the gain. Their data shows that the gain is dependent on the partial pressures of the methyl cyanide and water vapour in the amplifier cell, and also on the discharge current . Similar work has been done by Stafsudd and Yeh (Ref.15), who studied methyl cyanide as well as mixtures of methane and nitrogen. The highest gains, in both cases, are in the region of 7-11% per metre. Stafsudd and Yeh also measured the radial dependence of the gain and found, within experimental error, the gain to be independent of the radius. This radial behaviour was found for both 5 and 7.5cm diameter tubes. The gain was also independent of the wall temperature in the measured range of 0 to 100°C. However, the gain was found to increase linearly with the flow rate of the gas for a constant pressure and current in the discharge tube. The flow rate of the gas was varied within the range 0 to 28cc/min (at STP) of methyl cyanide. Faster flow rates could not be obtained with the system used and consequently the saturation of this effect was not observed.

The active material in this type of laser gets 'used up' forming a thick polymer deposit on the walls and can no longer contribute to the gain. This would suggest that increasing the flow rate of the gas would simply increase the distance the molecules could travel before forming the polymer, in other words the effective length of the active region is increased. Hence it is possible that the gains/metre quoted in Refs. 14 and 15 are not the true gains/metre, but that most of the gain is only in a certain length from the point where the gases enter the discharge tube.

2.5 Operating Mechanism of the HCN Laser

Chantry et al. (Ref.25) suggested a theory for the 337μm laser line in which the lasing transition was identified as a rotational transition in the vibrational state v = 2 of the electronic ground state of the CN radical. The population inversion is explained by the presence of one of the rotational perturbations which involve the first and second excited electronic states of CN ($A^2\Pi$ and $B^2\Sigma$). There are four rotational perturbations between the $A^2\Pi$ v=10 and $B^2\Sigma$ v=0 states involving the k = 4, 7, 11 and 15 rotational levels respectively. These rotational levels in the $B^2\Sigma$ state are hence excited by the $A^2\Pi$ state which is selectively excited in an electrical

discharge. Considering the k = 7 rotational level, it was suggested that because of the strict selection rule $\Delta k = \pm 1$, the P-branch of the electronic transition from the $B^2\Sigma$ v=0 to the $X^2\Sigma$(ground) state would populate the k = 8 rotational levels while leaving the k = 7 levels essentially unpopulated. These rotational levels in the v = 2 vibrational state correspond to the 337μm laser transition. The inversion mechanism suggested in this theory explains the failure to obtain laser oscillations with compounds containing C^{15}. Isotopic changes in the molecule would result in a significant change in the vibrational energies, thus altering the perturbation conditions of their rotational levels.

Broida et al. (Ref.26) pointed out that, if the model proposed by Chantry et al. was correct, then a number of other transitions should oscillate - some with higher probabilities than that of the 337μm transition. If the P-branch of the $B^2\Sigma$ v=0 to $X^2\Sigma$ v=2 transition inverts the population in the lower state, then the R-branch would also be expected to do so, and in principle, this mechanism should also apply to the other three rotational perturbations at k=4, 11 and 15. There is also a possibility of the corresponding rotational levels in the v=1 and v=0 levels of the $X^2\Sigma$ state being inverted. In addition, the radiation relaxation rate of the $B^2\Sigma$ state is a factor of 50 times the collisional rate of rotational relaxations. This

suggests that the selective excitation of the k = 4, 7, 11 and 15 rotational levels in the $B^2\Sigma$ state should also result in four rotational laser transitions, to the corresponding lower rotational level. Only one of the many transitions predicted by Broida et al., at 538μm, has been observed. Oscillations at this wavelength were obtained by Steffen et al. (Ref.8) in a pulsed discharge through ICN. Another obvious criticism of the theory of Chantry is that it fails to explain the effect of hydrogen on the lasing transition since, as has been observed (Ref.6), a different spectrum of laser lines is obtained when deuterium is substituted for hydrogen.

The rotational transition from k=8 to k=7, in the $X^2\Sigma$ v=2 state, is a spin doublet and support was given to the theory of Chantry et al. by the report of laser oscillations on both members of the doublet by Camani et al. (Ref.24). However, Hocker et al. (Ref.21) put forward two objections. First in contradiction to the proposed scheme, on the application of magnetic fields up to 800 gauss, no Zeeman broadening was observed in the laser line width. Secondly, frequency measurement showed no indication of two separate laser transitions around 337μm, suggesting that Camani may have wrongly identified different resonator modes of the same transition as two separate transitions.

Steffen et al. (Ref.4 and 27) have put forward two separate theories for the lasing mechanism. In the first theory the

laser transitions are identified with vibrational-rotational transitions between the $X^2\Sigma$ and $A^2\Pi$ states. The 311μm and 337μm transitions are linked in a cascade which starts and ends in the same v = 11 vibrational level of the $X^2\Sigma$ state with a common level in the $A^2\Pi$ state. This allows the sum of the two transitions to be worked out from the accurately known rotational constants only. The resulting error of $2cm^{-1}$ (Ref.21) completely rules out this identification. For the second theory by Steffen et al. (Ref.27) work was done with the help of a digital computer which fitted the laser transitions to transitions in the CN spectrum. The 311 and 337μm lines are placed as vibrational-rotational transitions between the $A^2\Pi$ and $B^2\Sigma$ states of CN. This identification is unlikely because low populations would be expected in the high vibrational and low rotational levels which are involved in the scheme. Typical values are 18 and 3 respectively. Also the low J quantum numbers would be expected to show a relatively large Zeeman splitting which has not been found by Hocker et al. (Ref.21).

Finally, the cascade properties of the laser, involving the 311μm, 337μm and four other transitions, which have been studied by Hocker and Javan (Ref.22) do not fit any of the proposed identifications.

Lide and Maki (Ref.28) have worked out a theory for the laser in terms of the spectrum of the HCN molecule. The fit between the calculated and observed laser transitions is

excellent, and in addition the theory has been able to explain most of the properties of the laser.

2.6 Theory of Lide and Maki for the HCN Laser

Lide and Maki (Ref.28) have explained four lines, including the intense 337μm line, as transitions involving the $11^1 0$ and $04^0 0$ vibrational levels in the ground state of the HCN molecule. These transitions (ν_a, ν_b, ν_c and ν_d) are shown in Fig.1. The population inversion between these vibrational states is explained by postulating that vibrationally excited HCN is formed in the discharge, the excitation being in the ν_1 normal mode (see Fig.3). This scheme would not work under normal conditions for two reasons:

a) The transitions ν_a and ν_b, belonging to a combination band, would have extremely small transition probabilities because a many quantum jump is involved.

b) Collisional relaxation among the rotational levels would make it difficult for a population inversion to be established in the case of the ν_c and ν_d transitions.

However, there is a Coriolis perturbation between the $11^1 0$ and $04^0 0$ states due to the near degeneracy of the rotational levels at J=10. This results in a considerable mixing of the two vibrational states at the J=10 level. To a lesser degree, the states are also mixed at the J=9 and J=11 levels. As the

transition probability of the pure rotational transitions is high, this mixing results in a considerable enhancement of the transition probabilities for the vibrational-rotational lines ν_a and ν_b. Consequently, with a population inversion between the 11'0 and $04^0 0$ states, the transitions ν_a and ν_b could be made to oscillate.

Probably because of the relatively fast relaxation between rotational levels, the transitions ν_c and ν_d have only recently been observed in continuous operation of the laser (Ref.22). In fact, ν_c and ν_d can only oscillate continuously when the 337μm (ν_a) line is oscillating. The lines ν_e and ν_f, which were discovered after the paper by Lide and Maki, can also oscillate continuoully only when the 311μm (ν_b) is oscillating.

In a later paper Maki (Ref35) has assigned four more transitions to higher levels in the HCN molecule, a further two laser transitions being predicted. The vibrational states involved are $12^0 0$, $12^2 0$ and $05^1 0$. In a scheme similar to the previous one described, the levels are mixed by Coriolis perturbations. The $12^{2d} 0$ and $05^{1d} 0$ states cross at the J=26 level and the $12^0 0$ and $05^{1c} 0$ levels cross at the J=25 level (Fig.2). Mixing of these levels again allows the otherwise weak vibrational-rotational transitions to gain some of the intensity of the pure rotational transitions. The observed and predicted values for these transitions, as well as the transitions

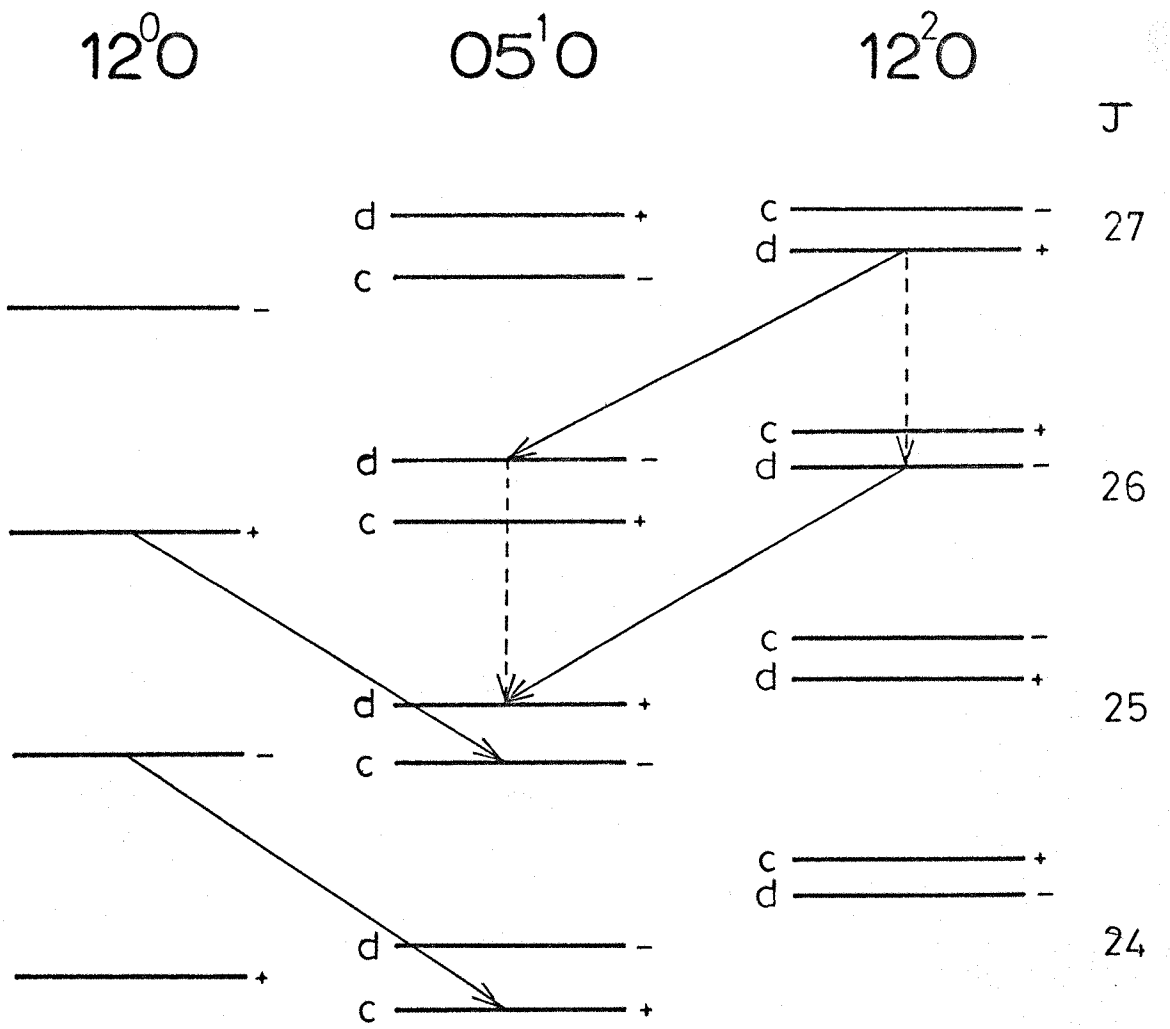

FIG. 2. Solid lines show observed and dashed lines show predicted laser transitions.

involving the $11^{1}0$ and $04^{0}0$ states are tabulated in Table 2. The close fit between theory and experiment can be seen.

2.7 Q-switching of the HCN Laser

Besides the primary objective of achieving high peak powers, the HCN laser was Q-switched to obtain information on the lifetimes of the levels associated with the laser transitions (Ref.23) A rotating mirror was used and, in addition to the resonant cavity formed with this, a second cavity was formed at an adjustable angular position of the mirror by means of a third mirror. With this arrangement two laser pulses are obtained for every revolution of the mirror, the time interval between the pulses depending on the mirror speed. During the experiment it was found that, as the mirror speed was increased, the laser pulses narrowed in width and increased in intensity. For the 337μm transition a power increase of five was obtained over the CW condition. This indicated that the inversion mechanism of the HCN laser was capable of energy storage. With a steadily increasing mirror speed, both laser pulses reached a maximum intensity and then the intensity of the second pulse started to decrease. Higher speeds decreased the intensity of the first pulse as well and, at the maximum mirror speed of 500 rev/sec, the pulse occured only on alternate mirror revolutions.

Table 2

Observed and Calculated Laser Lines for the HCN Molecule

From Ref. 28 and 35.

Upper state	Lower state	Observed cm^{-1}	Calculated cm^{-1}
$11^{1}0$ J=10	$04^{0}0$ J=9	29.7125[a]	29.712
$11^{1}0$ J=11	$04^{0}0$ J=10	32.1660[a]	32.172
$04^{0}0$ J=9	$04^{0}0$ J=8	26.8436[a]	26.845
$11^{1}0$ J=11	$11^{1}0$ J=10	32.2878[a]	32.289
$04^{0}0$ J=10	$04^{0}0$ J=9	29.8344[a]	-
$11^{1}0$ J=12	$11^{1}0$ J=11	35.21[a]	-
$12^{2d}0$ J=27	$05^{1d}0$ J=26	79.262	79.259
$12^{2d}0$ J=27	$12^{2d}0$ J=26	-	79.455
$12^{2d}0$ J=26	$05^{1d}0$ J=25	77.743	77.749
$05^{1d}0$ J=26	$05^{1d}0$ J=25	-	77.936
$12^{0}0$ J=26	$05^{1c}0$ J=25	76.430	76.415
$12^{0}0$ J=25	$05^{1c}0$ J=24	74.111	74.093

a - from Hocker (Ref.22)

To interpret the behaviour of the pulses and to calculate the transition probabilities of the laser levels Frayne (Ref.23) proposed a mathematical model for the Q-switching experiment. The following assumptions were made in deriving an expression for the population inversion as a function of time after a Q-switch pulse:

1. The upper laser level is pumped at a constant rate W/sec.
2. In the misaligned cavity, the transition probability (γ_A) for the decay of the upper state population, has a radiation contribution γ_a and a collisional contribution γ_o.
3. Similarly, the lower laser level has a total transition probability γ_B ($= \gamma_b + \gamma_1$).
4. The condition for continuous laser operation is $\gamma_a < \gamma_B$.
5. The lower laser level is only populated by the radiative transitions from the upper state, i.e. the population of the lower level by all other mechanisms if neglected.
6. A Q-switch pulse completely depletes the population inversion.

The expression obtained in ref.23 for the inversion at a time t after depopulation is :

$$N(t) = \frac{W}{\gamma_A}\left[1 - \frac{\gamma_a \gamma_B}{\gamma_B(\gamma_A - \gamma_B)}\right] - \frac{W}{\gamma_A}\left(1 + \frac{\gamma_a}{\gamma_B - \gamma_A}\right)\exp(-\gamma_A t) - \frac{\gamma_a}{\gamma_b}\exp(-\gamma_B t) \quad \ldots\ (2.7.a)$$

The derivation of this expression is not understood as, starting with the same assumptions as above, a different form for the expression has been obtained. Substituting $t = \infty$ in the above expression gives the steady state inversion as

$$N(\infty) = \frac{W}{\gamma_A} \quad 1 - \frac{\gamma_a \gamma_A}{\gamma_B(\gamma_A - \gamma_B)}$$

This is not the usual expression for the steady state inversion with this model. Also if $\gamma_A = \gamma_B$, $N(\infty) = -\infty$ which implies that the population of the upper state is infinite, a surprising result.

The rate equations for the upper and lower levels respectively are :

$$\frac{dN_A}{dt} = W - N_A\gamma_A \qquad \ldots\ (2.7.b)$$

and

$$\frac{dN_B}{dt} = N_A\gamma_a - N_B\gamma_B \qquad \ldots\ (2.7.c)$$

At the steady state ($t = \infty$) :

$$N_A(\infty) = \frac{W}{\gamma_A} \qquad \ldots\ (2.7.d)$$

and

$$N_B(\infty) = \frac{W\gamma_a}{\gamma_A\gamma_B} \qquad \ldots\ (2.7.e)$$

Hence considering the assumption (6) above, the initial populations of the levels are ($t = 0$) :

$$N_o = \frac{N_A(\infty) + N_B(\infty)}{2}$$

$$= \frac{W}{2\gamma_A}\left(1 + \frac{\gamma_a}{\gamma_B}\right) \qquad \ldots\ (2.7.f)$$

Solving (2.7.b) with the initial condition (2.7.f) gives :

$$N_A(t) = \frac{W}{\gamma_A} - \frac{W}{2\gamma_A}\left(1 - \frac{\gamma_a}{\gamma_B}\right) \exp(-\gamma_A t) \qquad \ldots\ (2.7.g)$$

This value of N_A is substituted in (2.7.c) and the equation is also solved with the initial condition (2.7.f) :

$$N_B(t) = \frac{W\gamma_a}{\gamma_A\gamma_B} - \frac{W\gamma_a(\gamma_B - \gamma_a)}{2\gamma_A\gamma_B(\gamma_B - \gamma_A)} \exp(-\gamma_A t)$$

$$+ \frac{W}{2\gamma_A}\left(1 + \frac{\gamma_a(\gamma_A - \gamma_a)}{\gamma_B(\gamma_B - \gamma_A)}\right) \exp(-\gamma_B t) \qquad \ldots\ (2.7.h)$$

From the equations 2.7.g and h, the inversion at a time t after the Q-switch pulse is obtained :

$$N(t) = \frac{W}{\gamma_A}\left(1 - \frac{\gamma_a}{\gamma_B}\right) - \frac{W}{2\gamma_A}\left(1 - \frac{\gamma_a}{\gamma_B}\right)\left(1 - \frac{\gamma_a}{\gamma_B - \gamma_A}\right) \exp(-\gamma_A t)$$

$$+ \left(1 + \frac{\gamma_a}{\gamma_B} \cdot \frac{\gamma_A - \gamma_a}{\gamma_B - \gamma_A}\right) \exp(-\gamma_B t) \qquad \ldots\ (2.7.i)$$

The steady state inversion is given by ($t = \infty$) :

$$N(\infty) = \frac{W}{\gamma_A}\left(1 - \frac{\gamma_a}{\gamma_B}\right) \qquad \ldots\ (2.7.j)$$

This is the usual expression for the steady state inversion with this type of model and clearly gives the laser condition for

$\gamma_B > \gamma_a$.

The inversion can be expressed as a fraction of the final inversion:

$$\frac{N(t)}{N(\infty)} = 1 - \tfrac{1}{2}\left[\left(1 - \frac{\gamma_a}{\gamma_B - \gamma_A}\right)\exp(-\gamma_A t) + \left(1 + \frac{\gamma_a}{\gamma_B - \gamma_A}\right)\exp(-\gamma_B t)\right] \quad \ldots\ (2.7.k)$$

For the derivation of this expression it was found that assumption (5) was not necessary. A constant pumping rate αW, where α is some constant, for the lower laser level gave the same result.

Frayne explains the increase of the laser output, with increasing mirror speed, as due only to the manner in which the inversion is built up after a Q-switch pulse. From his equation (2.7.a) it can be seen that, if $\gamma_A > \gamma_B$, the inversion transiently overshoots its steady state value. Varying the mirror speed would result in laser pulses whose power would follow the transient form of the inversion i.e. as the mirror speed is steadily increased, the laser pulses reach a maximum power and then decrease again. An overshoot is obtained in the expression derived here (2.7.k), but the maximum value of this overshoot is estimated to be about 5% and occurs when $\gamma_A \simeq \gamma_B$. This is negligible compared to the factor of 5 overshoot over the steady

state inversion as claimed by Frayne.

Frayne proposed his explanation because, he says it is unlikely that the power increase in this laser is due to the normal Q-switching mechanism. The reason he gave was that the decay time of the photons in the aligned cavity (which he calculated to be 112ns) was short compared to the 5μsec alignment period at the highest mirror speed used. This statement would appear not to be valid considering the recent slow Q-switch experiments with ruby lasers (Ref. 57). It was shown that if a particular relation between the net gain per pass and the ratio of cavity transit time and shutter opening time is satisfied, a similar Q-switched pulse will be produced as that from a fast switched laser, so Frayne's postulated overshoot is not needed to explain the higher powers with the rotating mirror. At higher mirror speeds, the argument given by Frayne associates the decrease in intensity of the second pulse with the lifetime of the upper state. This would not be the case in normal Q-switching. The decrease in intensity, due to the repetition rate only, could be associated with either the upper or lower state lifetime.

In the only other report on the Q-switching of an HCN laser, Jones et al. (Ref.20) quote power increases of 2 to 3 times for the 337μm line. They attribute the decrease in the laser output, at higher mirror speeds, to the inability of the photon density to build up during the alignment period. This could be a factor

accounting for the decrease as accurate work (Ref.58), with a single mode Q-switched neodymium laser, has shown that the maximum power obtained depends critically on the mirror speed. The build up time is roughly estimated by considering that at $300^{o}K$, a thermal radiation of 3 photon/cc would be present in a cavity mode. This could take only 0.5μsec, with the value of the CW gain, to build up to a typical photon density of 10^{7}/cc. However, in the case of the HCN laser we cannot be sure that this is the only factor responsible. The lifetimes of the laser levels could also result in the decrease of power at high speeds. Hence simply varying the speed of rotation cannot give us any conclusive information about the lifetimes.

The optimum angular velocity of the rotating mirror could possibly be determined by spinning the mirror behind a shutter. The Q-switch pulse, on suddenly opening the shutter, would then be independent of the lifetimes of the levels. With this optimum angular velocity, variation of the repetition rate of the Q-switch could determine the longer lifetimes of the laser states. When the repetition rate approaches the lifetime of either of the states, the output power would start decreasing. Various repetition rates at the same angular velocity could be achieved by multiple-sided mirror blocks.

CHAPTER 3 SPECTROSCOPY OF THE HCN MOLECULE

3.1 Introduction to Linear Molecules

Polyatomic molecules are divided into different categories according to the shape of the molecule, i.e. the arrangement of the atoms. In general a molecule possesses several symmetry elements and hence must belong to a point group. The nomenclature used for the point groups in the theory of molecular structure is the same as that introduced by Schoenflies in the theory of crystal structure. Linear molecules belong to the point groups $D_{\infty h}$ or $C_{\infty v}$, depending on whether or not they have a plane of symmetry perpendicular to the internuclear axis. The molecule CO_2 is an example of the first case and HCN of the second.

The total energy of a polyatomic molecule is generally resolved, with the same approximation as in a diatomic molecule, into the sum of the rotational, vibrational and electronic energies. However, for polyatomic molecules this approximation has to be used with care, since there are frequent cases of the vibrational and rotational energies, and the vibrational and electronic energies being of the same order of magnitude. In these cases the interaction of the three kinds of motions would be much stronger than that encountered in diatomic molecules, and the approximation will not be very accurate.

The rotational energy levels of a linear molecule can be given by the same expression as that for the simple rotator in a diatomic molecule. This is true only if the molecule does not

possess any angular momentum about the internuclear axis. All known linear molecules in their ground state satisfy this condition and the levels are given by :

$$F(J) = BJ(J+1) - DJ^2(J+1)^2 + ...$$

where J is the rotational quantum number, $B = \frac{h}{8\pi^2 c I_B}$ is the rotational constant in which I_B is the moment of inertia about an axis perpendicular to the internuclear axis and passing through the centre of mass and is given by:

$$I_B = \Sigma m_i r_i^2$$

where r_i is the distance of the i^{th} atom of mass m_i from the centre of mass of the molecule

and D>>B is a constant which represents the influence of the centrifugal force which results in a very slight increase in the internuclear distance when the molecule is rotating.

If the linear molecule does possess an angular momentum about the internuclear axis, which is the case when the bending mode of vibration is excited, then the rotational levels are given by:

$$F(J) = B\left[J(J+1) - \ell^2\right] - D\left[J(J+1) - \ell^2\right]^2 + ...$$

where ℓ is the angular momentum associated with the bending mode of vibration and takes the values v_2, v_2-2,..... 1 or 0, where v_2 is the vibrational quantum number.

The term $-B\ell^2$ is generally included in the vibrational energy of the state being studied.

The rotational constant $B(=\frac{h}{8\pi^2 c I_B})$ has a slightly different value for the different vibrational levels, because the moment of inertia I_B changes during vibration in such a way that the average value of $1/I_B$ is not exactly the same as its value in the equilibrium position. For a linear triatomic molecule, the vibrational dependence of B is given by :

$$B_{v_1 v_2 v_3} = B_e - \sum_i \alpha_i (v_i + \tfrac{1}{2} d_i) + \sum_{ij} \gamma_{ij} (v_i + \tfrac{1}{2} d_i)(v_j + \tfrac{1}{2} d_j) + \gamma_{\ell\ell} \ell^2$$

where v_1, v_2, and v_3 are the quantum numbers of the three vibrational modes, v_2 being the degenerate bending mode.

$j \geq i = 1, 2, 3$ and $d_1 = 1$, $d_2 = 2$, $d_3 = 1$

The constant B_e is the value that B would have if the molecule was in its hypothetical equilibrium position. The constants $\alpha_i << B_e$ and $\gamma_{ij} << \alpha_i$ may be regarded as representing the main influence of the coupling between the rotational and vibrational motions.

The rotational levels of a molecule are classified as positive or negative depending on whether the total eigenfunction of the level remains unaltered or changes its sign with respect to an inversion at the centre of mass of the molecule. For the vibrationless ground state of linear molecules, the electronic and vibrational eigenfunctions remain unchanged by all symmetry

operations of the molecule, and consequently the symmetry character of the rotational level depends only on the rotational eigenfunction. The rotational eigenfunctions of a linear molecule are similar to the surface harmonics of a hydrogen atom, and from this the even rotational levels are positive, and the odd ones negative.

A rotational transision in a linear molecule can take place only if the molecule possesses a permanent dipole moment i.e. a molecule with a $D_{\infty h}$ symmetry cannot have a pure rotational spectrum. Also we have the selection rules :

$$\Delta J = \pm 1,$$

$$+ \longleftrightarrow - \text{ , } + \not\longleftrightarrow + \text{, and } - \not\longleftrightarrow -$$

The motions of the individual atoms in a vibrating polyatomic molecule are complicated and, unlike diatomic molecules, the atoms do not simply vibrate along the internuclear axis. However, any vibration of a polyatomic molecule can generally be resolved into a number of orthogonal vibrations called normal vibrations. The number of normal vibrations is equivalent to the number of vibrational degrees of freedom possessed by the molecule and, for a linear molecule, it can be easily shown that there are 3N-5 normal vibrations, N being the number of atoms in the molecule. For example, the HCN molecule has 9-5 = 4 normal vibrations, two of them being degenerate in energy. Fig.3 shows these normal

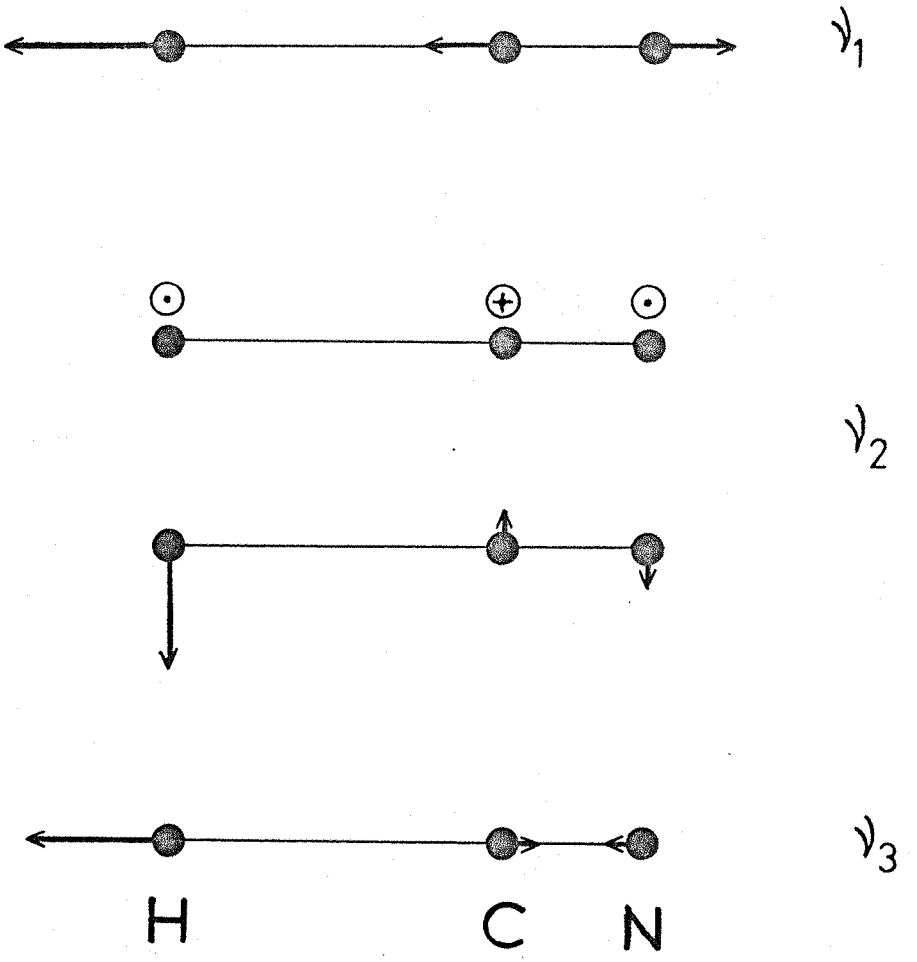

FIG. 3. Normal modes of vibration of the HCN molecule.

vibrations, the lengths of the arrows giving a rough idea of the amplitude of vibration of the different atoms.

For low vibrational numbers, the vibrational energies may be roughly estimated by assuming the vibrations to be harmonic. However, for accurate work, even in the case of fundamentals, quadratic and cubic anharmonic coefficients must be taken into account when determining the vibrational energies. For a linear triatomic molecule the vibrational energies are given by:

$$\begin{aligned} G(v_1, v_2, v_3, \ell) = & \sum_i \omega_i (v_i + \tfrac{1}{2}d_i) \\ & + \sum_{ij} x_{ij} (v_i + \tfrac{1}{2}d_i)(v_j + \tfrac{1}{2}d_j) \\ & + \sum_{ijk} y_{ijk} (v_i + \tfrac{1}{2}d_i)(v_j + \tfrac{1}{2}d_j)(v_k + \tfrac{1}{2}d_k) \\ & + \sum_i y_{i\ell\ell} (v_i + \tfrac{1}{2}d_i)\ell^2 + x_{\ell\ell}\ell^2 \end{aligned}$$

where $k \geq j \geq i = 1, 2, 3$

$$\begin{aligned} & d_1 = 1 \\ & d_2 = 2 \\ \text{and} \quad & d_3 = 1 \end{aligned}$$

The values of the coefficients used in this expression are generally obtained from accurate infra-red absorption measurements on the molecules.

The vibrational energy expression given above has been derived with an approximation that levels of each ℓ-value are doubly degenerate. This approximation is only valid for very low values of the rotational quantum number J, but breaks down for higher values of J when the levels are observed to be separate.

This is known as an ℓ-type splitting, the separation increasing with increasing J. On a classical basis there are two factors which can account for this splitting - different moments of inertia for the two vibrations and Coriolis interaction between the rotational and vibrational motions. Considering the first factor, the bending vibration in a linear molecule creates a small moment of inertia about the internuclear axis. The moment of inertia about an axis of rotation perpendicular to the plane of vibration will be the sum of this and the original moment of inertia. But the moment of inertia about an axis parallel to the plane of vibration will remain unchanged, to a first approximation, since during vibrations the atoms move parallel to the rotation axis. Consequently, because of the slightly different B values for rotation, a splitting of the levels will occur. The second factor is the Coriolis force which acts on the vibrating atoms of a rotating molecule. The dotted arrows in Fig.4 show the Coriolis forces acting on the atoms of an HCN molecule, the magnitude of the forces being given by:

$$F_{Cor} = 2mv\omega \sin \theta$$

where m is the mass of an atom and v its velocity in a co-ordination system locked to the rotating molecule,

ω is the angular velocity of rotation, and

θ is the angle between the axis of rotation and the direction of v.

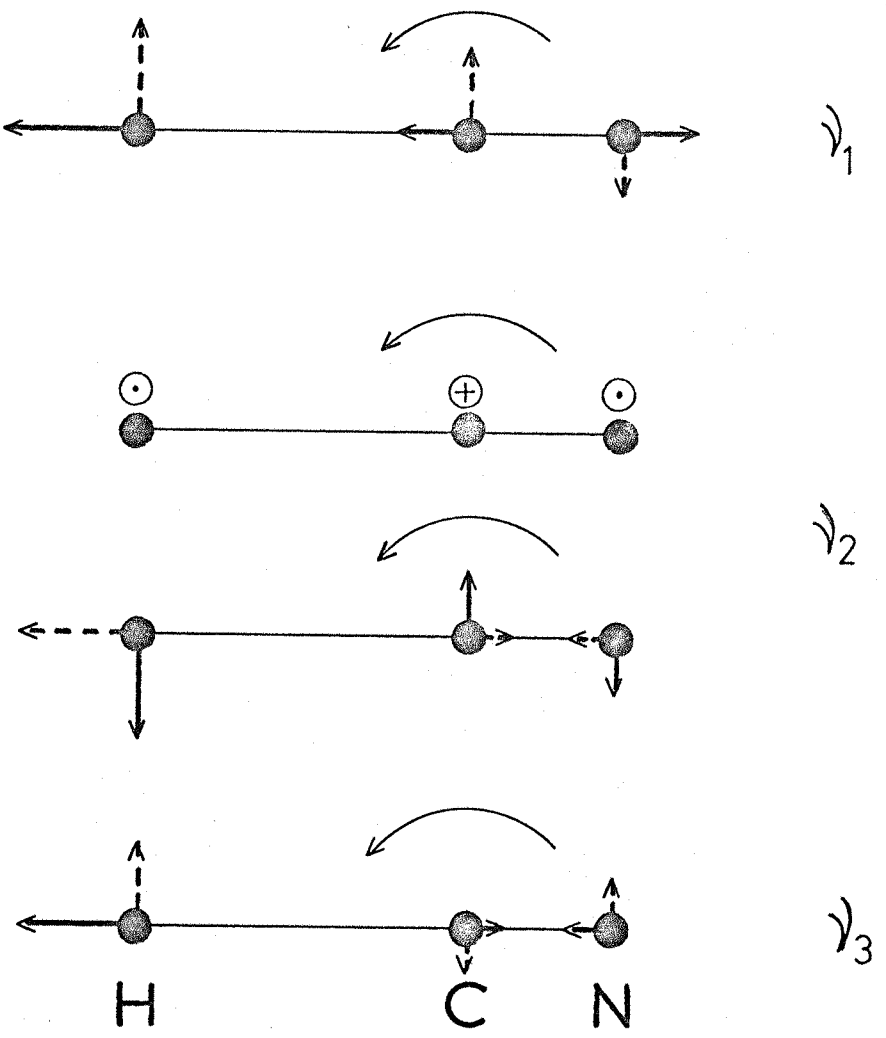

FIG. 4. Coriolis forces on a rotating HCN molecule.

From this it can be seen that only the vibration in a plane perpendicular to the axis of rotation will experience a Coriolis force. This causes the ℓ-splitting of the degenerate levels and, as the Coriolis force is proportional to the angular velocity, this splitting would be expected to increase with increasing J. Fig. 4 also clearly shows how a rotating molecule in the ν_2 mode tends to excite the ν_3 mode (with the frequency of ν_2) and vice versa. However, in practice the coupling between these vibrations is very small because the frequencies ν_2 and ν_3 are generally widely different. For the case of ν_1 the Coriolos forces do not correspond to another vibration, but are directed such as to produce a coupling with rotation.

The order of magnitude of the ℓ-splitting is such that the energy gap generally corresponds to microwave frequencies, the splitting being given by:

$$\Delta = q\, J(J+1)$$

where q is known as the ℓ-splitting constant.

A suitable choice for q generally gives a fair agreement with the observed values of the ℓ-splitting as determined from infra-red absorption measurements of the levels. However, these splittings have been directly measured ($\Delta J = 0$ transitions), by microwave spectroscopy, for many molecules, and because of the comparatively high accuracy achievable in microwave measurements,

this expression breaks down even for fairly low values of J. To explain this Amat and Nielson (Ref.36) took into account the effect of perturbation between the split vibrational levels differing by 2 in the value of ℓ, i.e. between the levels v, ℓ and v, $\ell \pm 2$. Maki and Lide (Ref.37), in their work on the HCN molecule, have shown that the additional perturbation between the levels v, ℓ and v, $\ell \pm 4$ must also be taken into account to explain the splittings accurately.

In the literature the two split levels are generally referred to as the c and d levels, with their own effective rotational constants B and D. The exact positions of the rotational levels can thus be directly calculated.

3.2 Details of the HCN Molecule

HCN is a linear triatomic molecule belonging to the point group $C_{\infty v}$ i.e. it has an ∞-fold axis (along the line joining the nuclei) and an infinite number of reflection planes through this axis. Fig. 5 gives a rough indication of the positions of the different vibrational levels of HCN in its ground electronic state. Rank (Ref. 38) has performed a detailed analysis of the spectrum of the HCN molecule and has determined most of the vibrational and rotational constants required to calculate the energies of the various levels. In a more recent paper Maki and Blaine (Ref. 39)

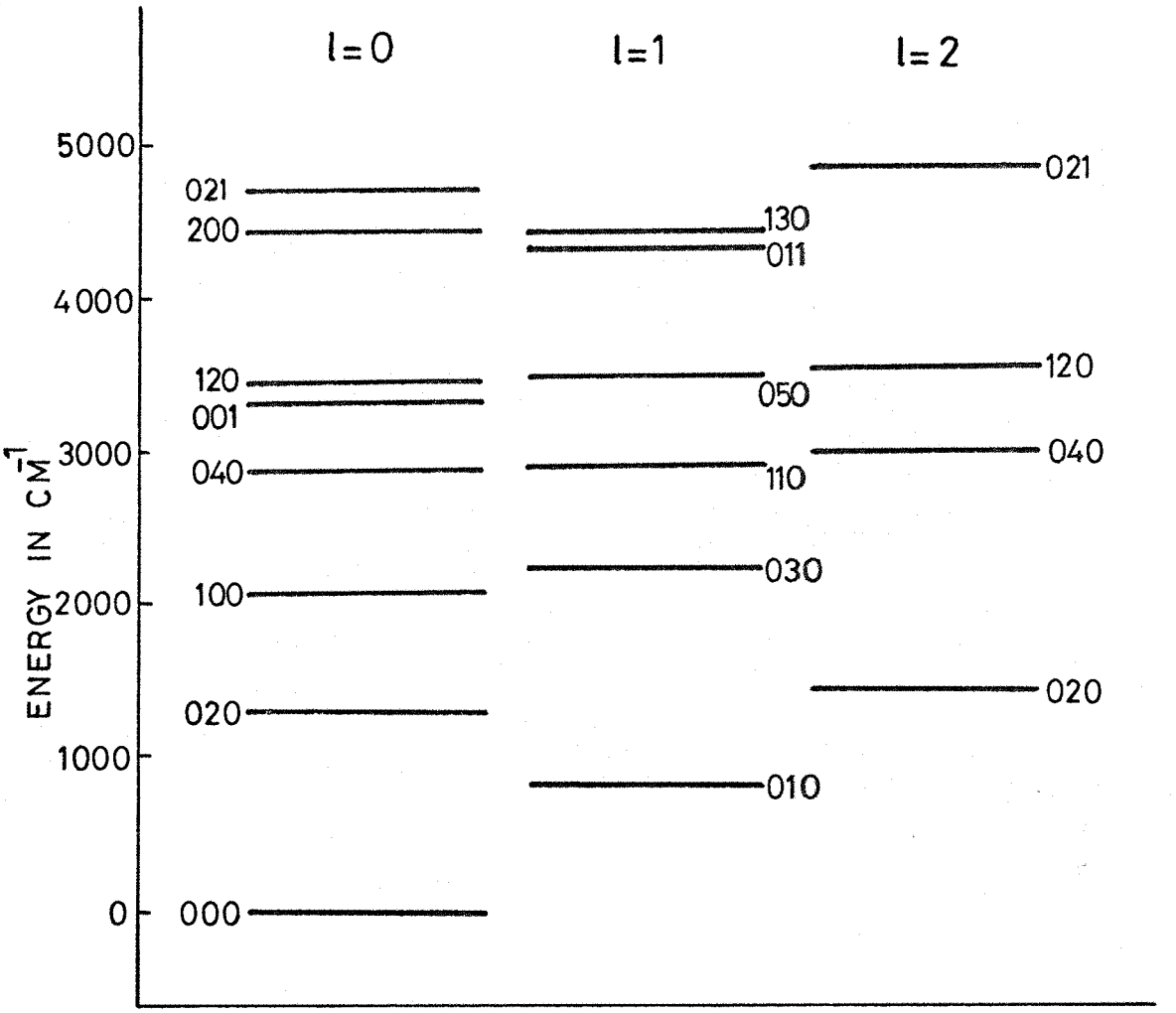

FIG. 5. Vibrational levels of HCN.

discharge through HCN. It was shown (Ref. 6) that this line can be obtained from numerous compounds as long as the three elements H, ^{12}C and ^{14}N are present.

The discovery of molecular lasers has made coherent sources available within the gap which existed between the near infra-red and microwave regions. With the numerous submillimetre laser lines known at present, there is no gap in the spectrum of coherent oscillation frequencies greater than about a factor of 1.5. The availability of fairly high powers, in a region where conventional spectrometers work on the 'tail' of the emission from a lamp, means that orders of magnitude greater sensitivity could be obtained for spectroscopic work. At present the molecular lasers are available at spot frequencies in the spectrum or may be tuned over a limited range (Ref. 53), and hence their application to spectroscopy is restricted to localized parts of the spectrum. Garrett (Ref. 54) has studied the application of submillimetre lasers to spectroscopic work, and has suggested that a technique similar to one used in electron spin resonance may be feasible. For example, in the investigation of far infra-red absorption lines (lying in the region of a submillimetre laser transition), the sample itself may be tuned across the laser line. This could be achieved by either a Zeeman or Stark shift which can be controlled by the application of magnetic or electric fields. It is seen that for practical pressures, and easily attainable

have re-analysed many of the bands and slight modifications for some of the constants have been given. The vibrational and rotational constants are listed in Tables 3 and 4 respectively. In addition, measurements were made on some new vibration-rotation bands and the effect of ℓ-type resonance was taken into account in working out the ℓ-splitting in the bending vibration mode. For the $_2$ band of the HCN molecule, the data published by Brim (Ref. 40) is accepted as the most accurate.

The rotational constants for the HCN molecule are known to a degree of accuracy that the rotational levels (up to fairly high J values) can generally be predicted to within less than $0.01 cm^{-1}$ of the observed position for most of the vibrational levels. However, owing to the complexity of the vibrations, the best fit for the vibrational constants, although predicting some levels with a fair degree of accuracy, gives the position of some levels a few wave numbers away from the observed position. The availability of data for the band centres of the different vibration-rotation bands is consequently essential for the accurate calculations of the rotational levels.

The laser transitions in the 300μm range can be calculated using the data available for the HCN molecule. The band constants for the $04^0 0$ state are taken from the microwave measurements of Maki and Lide (Ref. 37) and for the $11^1 0$ state from Maki and Blaine (Ref.39). Table 5 shows the rotational levels for these

TABLE 3

The Vibrational Constants for HCN

w_1	= 2119.8642	y_{111}	= -0.1889	$y_{1\ell\ell}$	= -0.099*
w_2	= 726.9950	y_{222}	= 0.0285	$y_{2\ell\ell}$	= 0.029*
w_3	= 3441.2207	y_{333}	= 0.2702	$y_{3\ell\ell}$	= -0.061*
		y_{112}	= -0.0012		
x_{11}	= -7.0741	y_{113}	= -0.7723	$x_{\ell\ell}$	= 5.255*
x_{22}	= -2.6533	y_{122}	= -0.0747		
x_{33}	= -52.4901	y_{133}	= -1.1010		
x_{12}	= -2.5265	y_{123}	= 0.1240		
x_{13}	= -10.4434	y_{223}	= -0.0375		
x_{23}	= -19.0055	y_{233}	= -0.1230		

Values taken from Rank et al. (Ref. 38)

* Denotes the values from Maki and Blaine (Ref.39)

TABLE 4

The Rotational Constants for HCN

B_e	= 1.484514	α_1	= 0.009673	11	= -0.00003
		α_2	= -0.00356*	22	= 0.00004*
		α_3	= 0.010441	33	= -0.000157*
				12	= -0.00012*
		$\alpha_{\ell\ell}$	= -0.00021*	13	= 0.000277*
				23	= 0.000223*

Values taken from Rank et al. (Ref.38)

*Denotes values from Maki and Blaine (Ref.39)

TABLE 5

The Unperturbed Rotational Levels of the $11^{1c}0$ and $04^{0}0$ States

J	$11^{1c}0$ cm^{-1}	$04^{0}0$ cm^{-1}
8	2911.248	2910.483
9	2937.660	2937.364
10	2967.004	2967.228
11	2999.281	3000.076
12	3034.488	3035.907

Constants used :

$B_{11^{1c}0} = 1.467809$ $\quad D_{11^{1c}0} = 2.94 \times 10^{-6}$

$B_{04^{0}0} = 1.493898$ $\quad D_{04^{0}0} = 3.341 \times 10^{-6}$

Band centres :

$11^{1}0 = 2805.58\ cm^{-1}$

$04^{0}0 = 2802.94\ cm^{-1}$

two states calculated directly with the constants.

The effects of perturbations are then taken into account. Considering first the $04^0 0$ state, the rotational levels are perturbed by the corresponding levels in the $04^2 0$ and $04^4 0$ states (Ref. 37). The perturbed $04^0 0$ levels can be determined by solving the secular determinant :

$$\begin{vmatrix} E_{\Gamma}^{o} - \epsilon & W_{42} & \sqrt{2}\, W_{40} \\ W_{42} & E_{\Delta}^{o} + W_{2_1-2} - \epsilon & \sqrt{2}\, W_{02} \\ \sqrt{2}\, W_{40} & \sqrt{2}\, W_{02} & E_{\Sigma}^{o} - \epsilon \end{vmatrix} = 0 \qquad \ldots (3.2.a)$$

This can be simplified by putting :

$$E_{\Delta}^{o} = E_{\Sigma}^{o} + \delta_o,$$

and $$E_{\Pi}^{o} = E_{\Sigma}^{o} + \delta_1,$$

where

$$\delta_o = 4\left[x_{\ell\ell} + \sum_i y_{i\ell\ell}(v_i + \tfrac{1}{2}d_i) - B_{\Delta} + \gamma_{\ell\ell} J(J+1)\right]$$

and

$$\delta_1 = 16\left[\,\,\,\,\right]$$

One of the roots of the resulting cubic equation in gives the perturbation energies of the rotational levels. The matrix elements and the constants used in this calculation are listed in Table 6.

The interaction constant for the Coriolis perturbation between the rotational levels of the $11^1 0$ and $04^0 0$ state has been obtained by Maki and Lide (Ref. 37). The observed position

TABLE 6

Constants for the 040 State of HCN

1. Matrix elements used :

$$W_{42} = q\left[J^2(J+1)^2 - 18J(J+1) + 72\right]^{\frac{1}{2}}$$

$$W_{2\ell-2} = 3\varrho J(J+1)\left[J(J+1) - 2\right]/2$$

$$W_{02} = (6)^{\frac{1}{2}} q\left[J^2(J+1)^2 - 2J(J+1)\right]^{\frac{1}{2}}/2$$

$$W_{40} = (6)^{\frac{1}{2}} \varrho\left[J^2(J+1)^2 - 18j(j+1) + 72\right]^{\frac{1}{2}} \times \left[J^2(J+1)^2 - 2J(J+1)\right]^{\frac{1}{2}}/2$$

2. $\varrho = -1.77 \times 10^{-8}\,cm^{-1}$

3. ℓ-splitting constant q :

For J = 8 = 78.1299×10^{-4}

J = 9 = 78.1125×10^{-4}

J =10 = 78.0933×10^{-4}

J =11 = 78.0721×10^{-4}

of the levels are thus obtained by using the expression:

$$\Delta^2 = \delta^2 + 4J(J+1)\ W_{ni}^{\ 2}$$

where Δ is the observed separation of the levels

δ is the calculated separation

and $W_{ni} = 0.0037\ cm^{-1}$, the interaction constant.

The calculated position of the rotational levels and the frequencies of the laser transitions obtained from them are shown in Table 7. The close fit between the observed and calculated value can be seen.

TABLE 7

Calculated Rotational Levels of the $11^{1c}0$ and $04^{0}0$ States of HCN

J	$11^{1c}0$ cm^{-1}	$04^{0}0$ cm^{-1}
8		2910.433
9	2937.663	2937.276
10	2966.989	2967.106
11	2999.278	2999.930
12	3034.488	

Observed and Calculated Laser Transitions

Upper level	Lower level	Observed (Ref.22)	Calculated
$11^{1}0$ J=10	$04^{0}0$ J= 9	29.7125	29.713
$11^{1}0$ J=11	$04^{0}0$ J=10	32.1660	32.172
$04^{0}0$ J= 9	$04^{0}0$ J= 8	26.8436	26.843
$11^{1}0$ J=11	$11^{1}0$ J=10	32.2878	32.289
$04^{0}0$ J=10	$04^{0}0$ J= 9	29.8344	29.830
$11^{1}0$ J=12	$11^{1}0$ J=11	35.21	35.210

CHAPTER 4 DETAILS OF EXPERIMENTAL WORK

4.1 Construction of the HCN Laser

4.1.1 The laser tube

The laser tube is sketched in Fig.6, the whole assembly being firmly supported on a 12 feet long steel girder. Internal mirrors were used and, to allow tilting of the mirrors for alignment purposes, bellows were fitted on either end between the laser tube and the mirror assembly. Initially one of the mirrors could be moved along the axis of the laser tube to tune the cavity length. It was however found that the cavity could be adequately tuned by slightly tilting one of the mirrors, and this procedure was subsequently used. The anode and cathode were both water-cooled and constructed of Dural. The main pyrex laser tube was cooked by a close-fitting copper strip jacket onto which cooling pipes were soldered. The anode was provided with a gas inlet pipe and the exhaust was through a 1" diameter tube at the cathode end. A flange was incorporated at the centre of the laser tube to allow windows of different materials, for example germanium, quartz or Irtran, to be held in place. With this arrangement it was possible to observe the sidelight from the discharge in the ultra-violet, visible and near infra-red regions.

The cathode presented some problems. Initially, a hollow cylindrical cathode, similar to the anode, was used along the

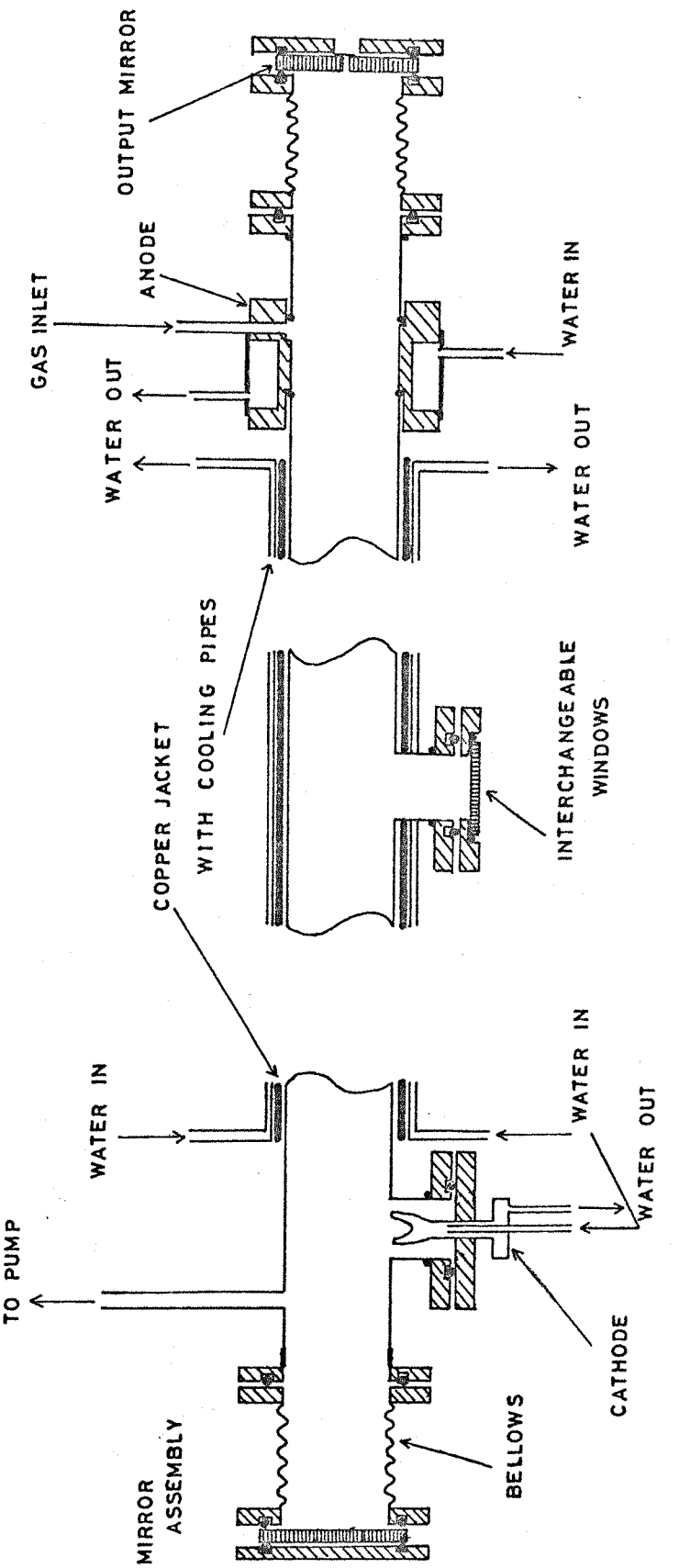

FIG 6 THE LASER TUBE

axis of the discharge tube. In this configuration the discharge could not be prevented from striking the mirror assembly at the cathode end. Insulating the mirror assembly from the cathode did not give any improvement. To overcome this the cathode was placed in a side-arm, a cylindrical U-shaped cathode giving the most stable discharge. The material of the cathode is also important because a stainless steel cathode produced excessive sputtering at the discharge currents normally employed. Dural electrodes were found to give considerably lower sputtering. Brass was the most satisfactory material, and it has been subsequently used for the cathodes.

4.1.2 The vacuum system

For laser operation the gas must flow continuously through the discharge tube. The system can be described as two separate parts, joined to the inlet and outlet respectively of the laser tube (see Fig.7).

a) The Gas-feed section: This consisted of two bottles A and B, each with a needle valve, connected through a flexible coupling to the inlet of the laser tube. A Pirani head was used to indicate the pressure. The gas inlet is at the anode end of the discharge tube and hence, to prevent a discharge to the metal parts of the gas-feed system, a 2.5 metre long glass tubing was interposed between the laser tube and the metal vacuum tubing. The bottles A or B contained organic liquids,

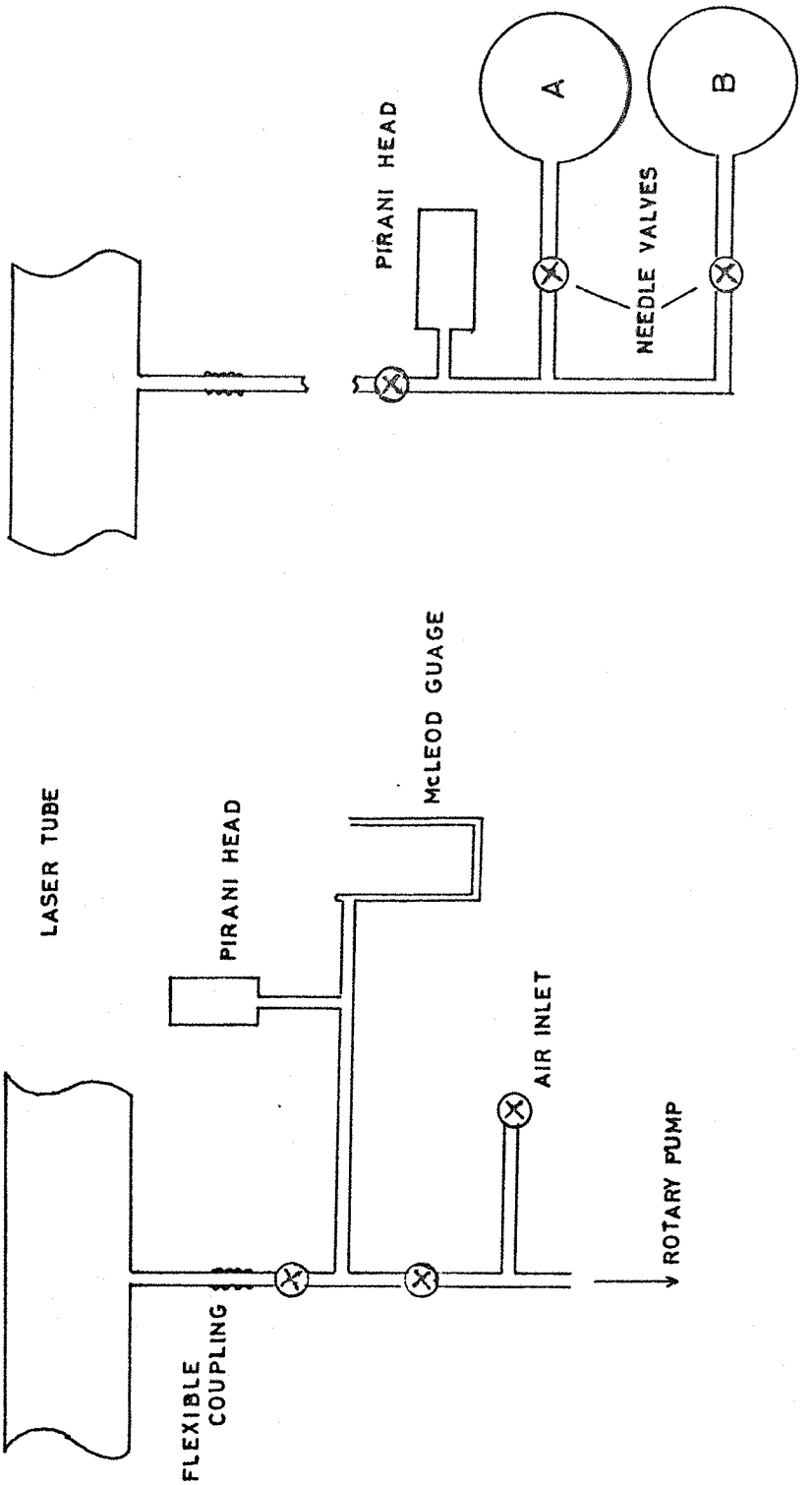

FIG. 7. THE VACUUM SYSTEM

for example methyl cyanide, the vapour being pumped through the discharge tube on opening the needle valve. During operation of the laser, evaporation causes a drop in the temperature of the liquid and hence, to maintain a constant pressure in the laser tube, the needle valve must be periodically adjusted.

b) Gas exhaust section : This consisted of an Edwards ED250 rotary vacuum pump connected through a flexible coupling to the outlet of the discharge tube. The pump had a maximum pumping speed of 250 litres/min, and the exhaust section was constructed with 1" diameter tubing to present minimum obstruction to the gas flow. With this pump an ultimate pressure of about 10^{-3} torr could be achieved. A McLeod gauge as well as a Pirani gauge, were used for measuring the pressure.

Because of the possibility of toxic concentrations of HCN being formed in the discharge tube and exhausted by the pump, the output from the pump was released outside the laboratory.

4.1.3 The power supply

The power supply was constructed using a 3-phase full-wave rectifier bridge employing 6 STC872A mercury vapour rectifiers. The supply was designed to give a continuous current of 1.5 amps at a voltage of 3.5kV. The complete circuit of the supply is shown in Fig.8. Power to the main transformer is controlled by

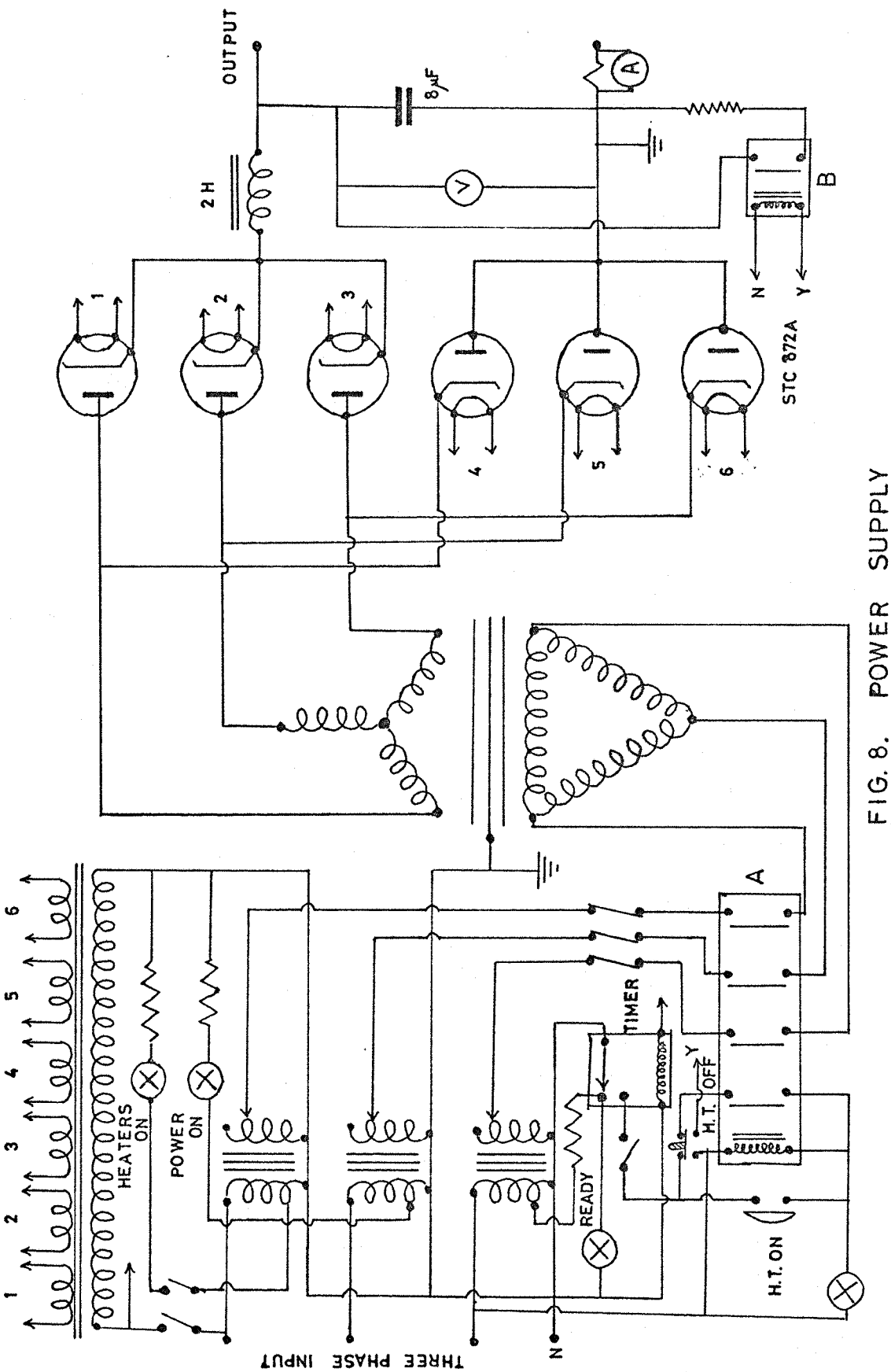

FIG. 8. POWER SUPPLY

contactor A. This contactor cannot be energized for a period of about 4 minutes after the filaments of the rectifiers have been switched on. This timing circuit is to avoid accidentally switching on the high tension before the mercury-vapour tubes have warmed up - the minimum time specified for them is about 3 minutes. In addition, contactor A cannot be closed unless the main variac is at its zero voltage position, a microswitch being depressed at this position. This feature ensures that a high setting of the high tension is not suddenly switched on, but that the voltage at the time of switching on is always zero. Contactor B is connected in such a way that it is held closed whenever the HT off button is pressed. In the closed position, contactor B connects a resistance across the smoothing capacitor and discharges it.

The output voltage from the supply has a ripple of about 1.5%. This was measured with the supply delivering 0.5 amps into a 3kΩ load. During operation of the discharge tube, the power supply is connected to the electrodes through a ballast resistance which could be varied from 3-10kΩ.

4.1.4 The resonator

Because of the long wavelength of the laser line the resonator requirements are not very critical. The mirrors used for the resonator can be crude compared to optical standards when we consider that the wavelength of the laser is roughly a factor

of about 600 longer than optical wavelengths. However fairly large diameter laser tubes and mirrors have to be used to avoid diffraction losses. According to the work of Li (Ref.29), for a mirror Fresnel number of 0.7 a diffraction loss of 1% per pass would be obtained. For the 337μm wavelength and a cavity length of 2.5 metre, mirrors of 5cm diameter would hence be required to give less than 1% per pass diffraction loss. For most of the work reported here 7.6cm diameter mirrors were used, corresponding to a Fresnel number of 1.7 with a 2.5 metre long cavity. A spherical-spherical mirror configuration was generally used with mirrors of 3 metre radius of curvature. The mirror substrates were glass and a coating of aluminium was deposited on them. For protection of the aluminium coating, a thin layer of silicon monoxide was deposited on the finished mirror.

Power was coupled out of the resonator by a hole in the centre of one of the mirrors. The hole was sealed by either a thin slice of quartz or Melinex (a polythene product of ICI). The power coupled out from the hole was estimated from the data of McCumber (Ref.30). For a 1.5mm hole in one of the mirrors of a spherical-spherical configuration, roughly 0.6% of the power in the cavity is coupled out at 337μm. Small diameter coupling holes were always used in this project because low threshold currents for laser operation were required rather than the higher output power which could be obtained from larger coupling holes.

One of the mirrors was designed to move along the axis of the tube to alter the resonator length. This was done because the line width associated with the transition is about 8MHz whereas the axial mode separation of the laser resonator was of the order of 60MHz for a 2.5 metre length. In practice it was found that the laser oscillated on a number of radial modes in addition to the axial modes. Since many radial modes lie between the axial modes, the tuning requirements are considerably reduced. Experimentally it was found that tilting one of the mirrors was just as effective in bringing the laser into oscillation as tuning the length of the resonator.

4.1.5 Output detection system

A 'Unicam' Golay cell with a diamond window was used to detect the output from the laser. The laser output was mechanically chopped at 11Hz to suit the time constant of the detector and the output from the detector was displayed on a millivoltmeter after phase-sensitive detection in the associated electronics. For an indication of the wavelength, the laser output could be passed through a Bausch and Lomb monochromator which was fitted with a 1.67 lines/mm far infra-red grating blazed at 310μm. The laser beam could be directed and focussed by means of front surfaced mirrors and polythene lenses. The monochromator was calibrated by using the higher orders of a He-Ne laser operating at 6328Å, and the calibration curve is reproduced in Fig.9. The monochromator was of a design for working in the visible region

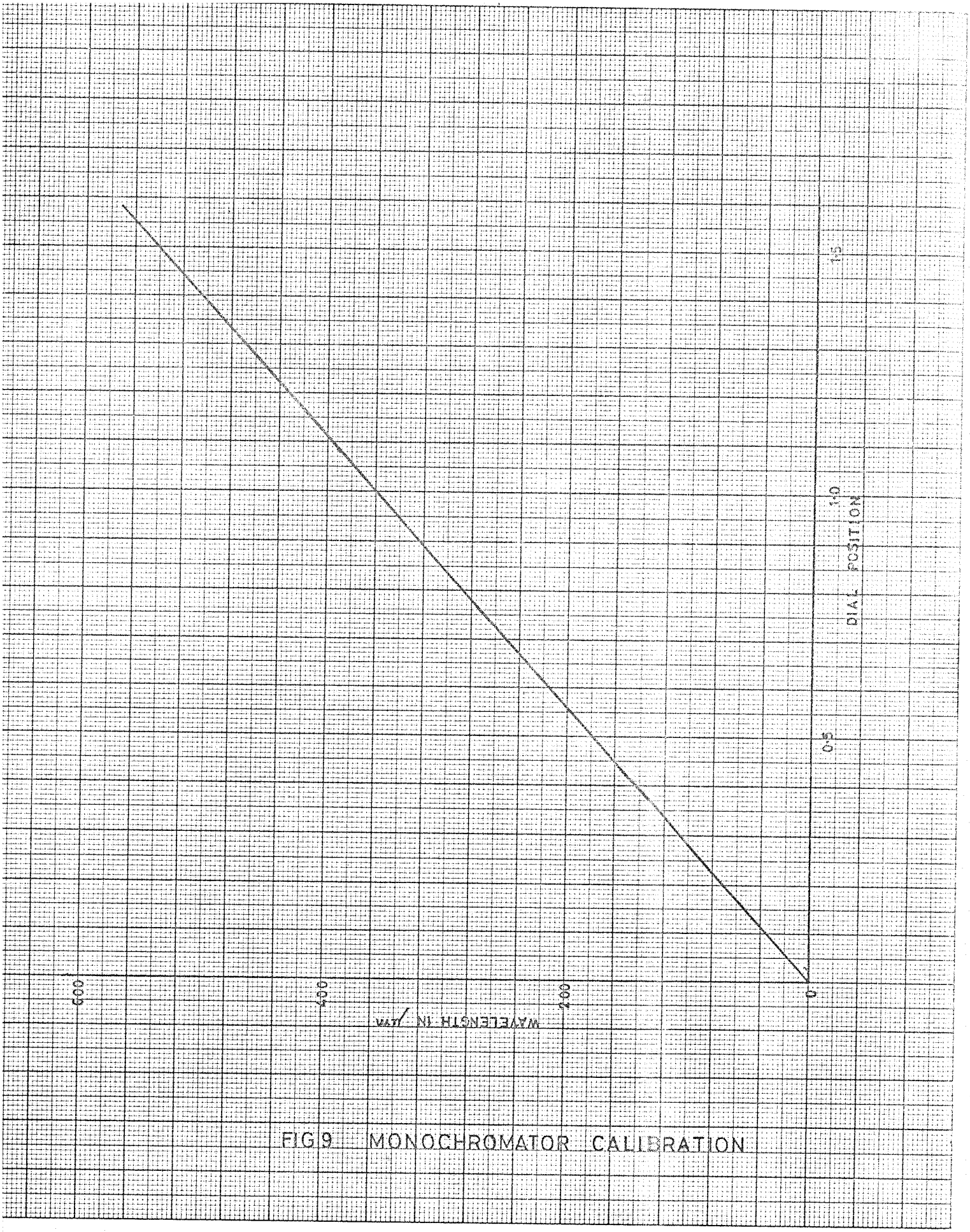

FIG 9 MONOCHROMATOR CALIBRATION

and hence an accuracy of only ±2μm could be obtained for the far infra-red wavelengths. This was however sufficient for our purposes as only an indication of the lines, on which the laser was oscillating, was required.

4.2 Spectroscopic Observation of the Side-Light from the Discharge Tube

At the start of this project, three separate theories (Ref. 4, 25 and 27) existed for the mechanism of operation of the so-called CN laser. In all the theories the 337μm and other prominent laser lines were assigned to transitions in the CN molecule, but in different parts of the spectrum. None of these assignments seemed valid (Ref. 21 and 26), suggesting that some other molecule may be responsible for the laser action. In an attempt to identify the lasing species, a spectroscopic study of the side-light emission from the discharge tube was proposed. Waksburg and Carswell (Ref.41) have shown that it is possible to identify the levels associated with a lasing transition from an analysis of the side-light spectrum. Helium-neon and carbon dioxide lasers have been analysed in this way, and a similar scheme was proposed to search for the levels responsible for the laser oscillations in the 'CN' laser. The experiment depends on the influence of the laser oscillations on the populations of the various energy levels of the active medium. If A and B are

the upper and lower levels respectively of a lasing transition (Fig.10), then the intensity of any spontaneous transition having either A or B as one of the levels would depend on whether the laser is oscillating or not. For example, if the laser is oscillating the population of level A is relatively depleted with an enhancement of the population in level B. Consequently, the spontaneous transition 'a' would decrease in intensity and 'b' would have an increased intensity. Oscillation of the laser can be easily controlled by a mechanical chopper in the laser cavity. The search is made by scanning the side-light emission and a phase-sensitive detection system is used synchronised with the chopper in the laser cavity. This system would give an output when the side-light is fluctuating with the same frequency as the chopper. The success of this kind of experiment would, in general, depend on the position of the lasing levels. For example, if the levels are in an excited electronic state, the spontaneous emission searched for could be an electronic transition, the analysis of which can be completely simple.

The general lay-out of the experiment is shown in Fig.11. The monochromator was a 1-metre Hilger and Watts 'Monospek' instrument which, with suitable grating, was capable of working in the range 0.2-22μm. The range over which scanning was possible was limited by the detectors available. An RCA PI28 photo-multiplier covered the near ultra-violet and visible regions and

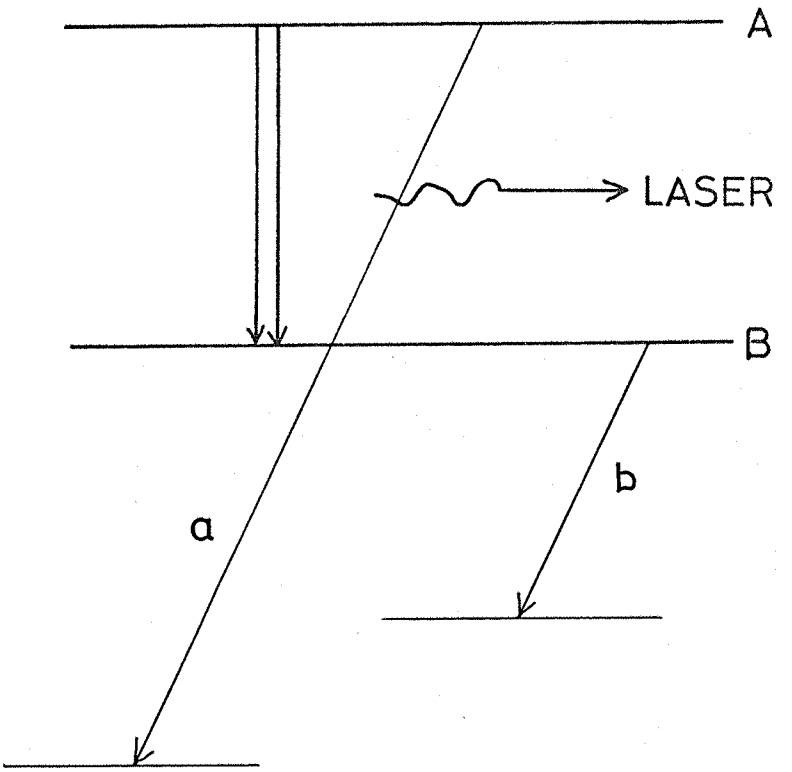

FIG. 10

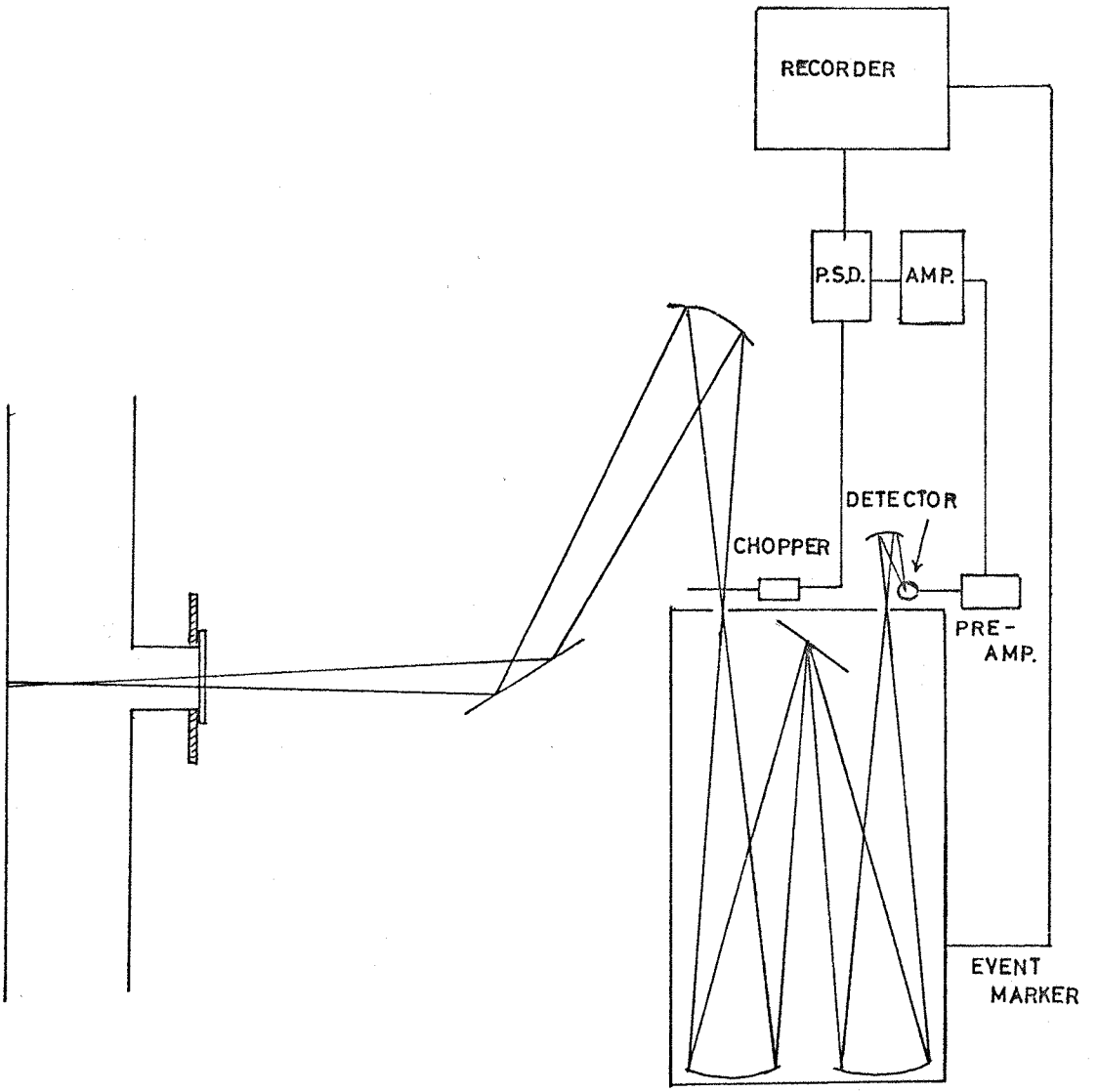

FIG. 11 SIDELIGHT DETECTION SYSTEM

a Mullards ORP13 indium antimonide detector could be used up to about 6μm. The ORP13 detector was of a liquid nitrogen cooled type and a low noise amplifier with a FET front end was built to amplify the signal. To minimise stray pickup, the first stage of the amplifier was incorporated into the detector housing. The amplifier was designed in the Electronics Department specially for use with the ORP13 (Ref.42), and the circuit diagram is given in Fig.12. The measured overall gain at 1Kz was 51.5db. Subsequent amplification and phase-sensitive detection was by a commercial 'AIM' system, and the output was fed into a 'Telsec' pen recorder. The recorder had provision for wavelength markers to be superimposed on the main trace when triggered by pulses from a cam-operated switch on the scanning drive of the monochromator.

To identify the lasing species it had been initially proposed to scan over as large a range as possible and search for intensity fluctuations of the spontaneous emission locked with the internal chopping of the laser. However, a paper by Lide and Maki (Ref.28) explained the laser in terms of the HCN molecule. The proposed theory explained many known properties of the laser and coupled with the accurate frequency measurements by Hocker et al. (Ref.21) gave a reasonable confirmation of the HCN molecule being the active species in the laser. Rough

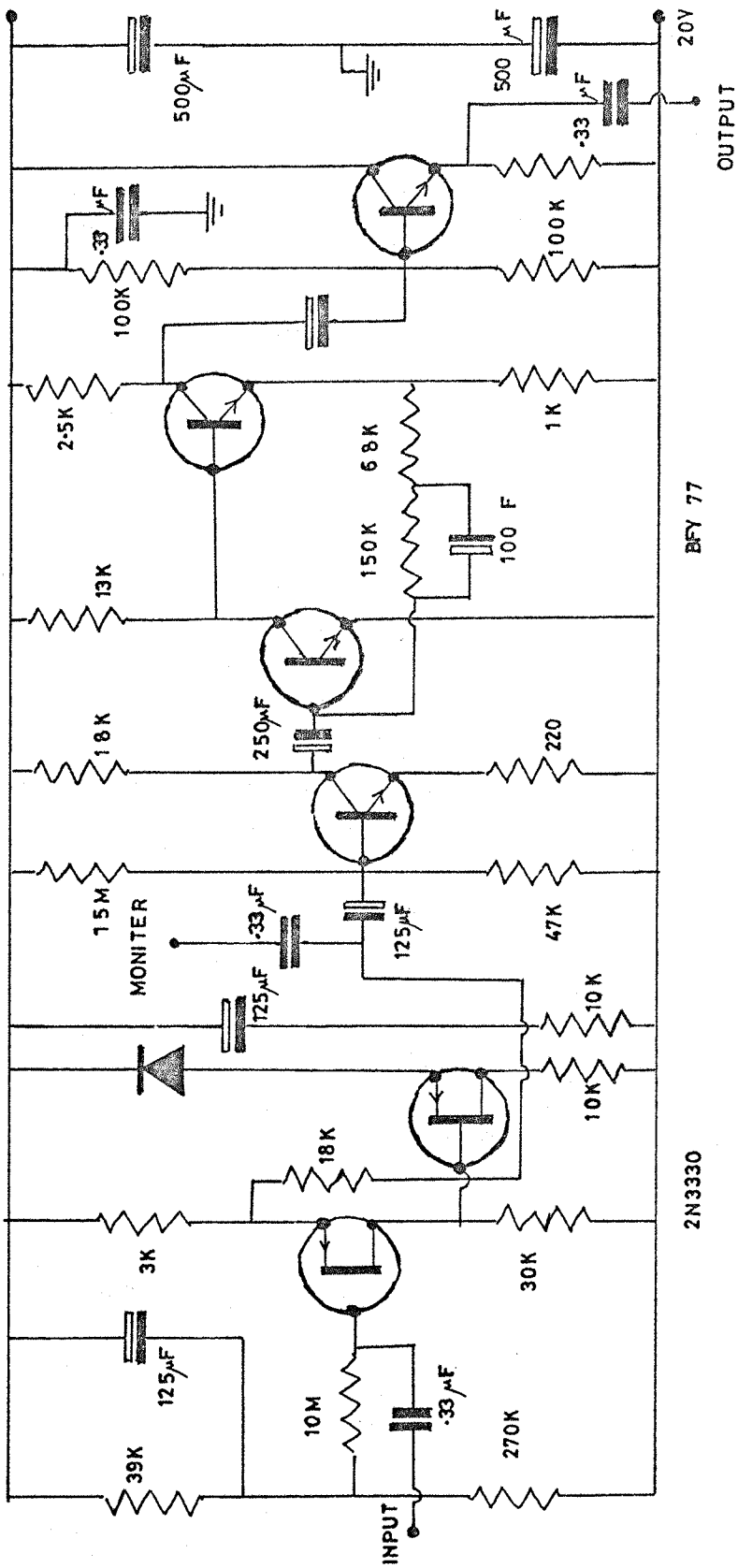

FIG. 12 LOW NOISE AMPLIFIER

calculations were made to determine the possibility of the application of the sidelight spectrum analysis to substantiate the theory by Lide and Maki.

The transition moments for the fundamentals of the HCN molecule can be obtained from the integrated absorption intensity measurements, of these vibrational-rotational bands, made by Hyde and Hornig (Ref.49). The integrated absorption intensity is related to the derivative of the dipole moment during a vibration:

$$A = \frac{N\pi}{3c^2}\left(\frac{d\mu}{dQ}\right)^2$$

where A, the integrated absorption, is in units of $cm^{-1}/cm.atmos$

N is the number of molecules of the gas in 1c.c. at NTP.

c is the velocity of light

and $\frac{d\mu}{dQ}$ is the derivation of the dipole moment with respect to the normal co-ordinates.

From this the transition moments for the vibrational bands can be roughly obtained by using the expression :

$$|R_{01}| = \left(\frac{h}{8\pi^2 \nu}\right)^{\frac{1}{2}} \frac{du}{dQ}$$

where R_{01} is the transition moment for the 0-1 band

and ν is the frequency of the transition.

Inserting values for the HCN molecule, we get the transition moments for the ν_1 and ν_2 fundamental bands.

$$|R_{01}|_{\nu_1} = 7.37 \times 10^{-21} \text{ c.g.s. units}$$

$$|R_{01}|_{\nu_2} = 1.13 \times 10^{-19} \text{ c.g.s. units}$$

Hence the transition probability for spontaneous emission of the first vibrational states can be evaluated:

$$(A_{10})_{\nu_1} = \frac{64\pi^4}{3hc^3} \nu_1^3 R_{01}^2$$

$$= 0.16 \text{ sec}^{-1}$$

and $(A_{10})_{\nu_2} = 1.45 \text{ sec}^{-1}$.

A total pressure of about 0.5torr of an organic mixture is typically optimum for laser action. We now assume that one half is converted into HCN in the 11^10 state, i.e. roughly 10^{16}molecules/c.c. of HCN are present in the 11^10 state. From the 11^10 state, considering the spontaneous transition probabilities given above, the transitions to the 100 state are expected to have the highest intensity. With the assumption that the probability for the 11^10 - 100 transition is equivalent to that of the 01^10 - 000 fundamental, the intensity of the spontaneous transition will be given by:

$$I(11^10\text{-}100) = N_{11^10} \cdot h\nu_2 \cdot (A_{10})_{\nu_2} \cdot 10^{-7} \text{ W/cc}$$
$$= 2 \times 10^{-4} \text{W/cc}$$

where N_{11^10} is the number of molecules/cc of HCN in the 11^10 state.

Taking into account the solid angle over which the radiation can be collected, and the losses in the optical system, a maximum intensity of roughly 10^{-7} watts can be expected to reach the detector on the output slit of the monochromator.

This rough calculation gives the integrated emission intensity over the $11^{1}0$ - 100 band, and the intensity of an indivisual vibrational-rotational line would be typically an order of magnitude lower. This intensity is getting close to the limit of the detection capability of the Golay cell, which has the highest detectivity in this wavelength region (about 14μm). If we now recollect the initial assumption, that one half of the organic material is converted into vibrationally excited HCN in the $11^{1}0$ state, we can conclude that a more realistic number of molecules in the $11^{1}0$ state would result in an emission intensity which could probably not be detected.

The lower limit on the number of molecules in the $11^{1}0$ state can be roughly estimated. The number of transitions/sec from the $11^{1}0$ J=10 state is obtained from the laser output. The number of transitions/sec is a product of the number of molecules in the $11^{1}0$ state, the Einstein B coefficient, and the radiation density in the cavity. For a 6mW laser output the radiation density in the cavity would be about 10^{-5} ergs/cc. From data on the HCN molecule, the B coefficient for the J=10 9 pure rotational transition in the $11^{1}0$ state, is evaluated as

5×10^{19} c.g.s units. From these values we set a lower limit of 10^{5} molecules/cc in the $11^{1}0$ state. This is a factor of 10^{11} lower than the number initially assumed in the calculation.

It should also be pointed out that the intensity fluctuations resulting from interupting the laser oscillations would not be restricted to the transition from the actual laser level, but would be spread out over most of the vibrational-rotational band. This would be due to the fast collisional relaxation of the rotational levels as compared to the long vibrational (radiative) lifetime.

The $11^{1}0$ - 100 band discussed above would be expected to have the greatest intensity of all the spontaneous transitions connected with the proposed laser levels of the HCN molecule. A transition involving a quantum jump in the ν_1 mode would have lesser intensity as would the transitions involving the lesser populated $04^{0}0$ state. The inability to detect the $11^{1}0$ - 100 transitions would imply that none of the other transitions, with orders of magnitude lesser intensity, could be detected. This kind of analysis, to determine the lasing mechanism, could thus not be used in the case of the HCN molecular laser. In addition, at this stage of the project, two papers were published (Ref. 21 and 22) which left little doubt about the assignment made by Lide and Maki (Ref.28) for the lasing transitions in the HCN molecule

The equipment being available, a few scans were made over the visible and the 3-5μm regions. The spectrum of the CN-radical was very prominent and in addition there were numerous unidentified bands. Irrespective of the starting materials in the discharge tube, for example methane-nitrogen, methly-cyanide etc., the CN spectrum could be easily obtained with very low discharge currents.

For a better understanding of the physical processes involved in the inversion mechanism of the HCN laser, a series of experiments were carried out in which some control, over the processes occuring in the laser tube, could be exercised. These experiments and their results are described in the succeeding sections.

4.3 Side-arm Experiment

The observation of CN, and many other unidentified species in a discharge through methane and nitrogen, together with the fact that the HCN laser oscillations can be produced with almost any compound containing H, ^{12}C and ^{14}N suggested that this may be a chemical laser, i.e. the HCN may be formed in the discharge in a vibrationally excited state. This would seem to follow from the observations of Gebbie (Ref. 5) where pure HCN was used and gave an output of the same order of magnitude as that from other mixtures containing H, C and N. From this the HCN

may first have to be dissociated before reforming in an excited state. Alternately, the formation of some excited dissociation product is essential to selectively transfer vibrational energy to the HCN molecule to invert the population. HCN itself is very easily formed as, referring to the literature on the behaviour of nitrogen in an electrical discharge, it is seen that nitrogen is very reactive with most hydrocarbons giving HCN as a primary product. Most of the available data on nitrogen reactions has been comprehensively compiled in a recent book by Wright and Winkler (Ref.43). Nitrogen that has been subjected to an electrical or r.f. discharge is generally referred to as 'active' nitrogen and contains the normal, and several excited, species of both N_2 and N. It is generally accepted that the N atoms, formed by the dissociation of the nitrogen molecule, react with the hydrocarbons to produce HCN. The reaction is fairly fast and the quantity of HCN produced when ethylene is introduced is one of the standard methods for the estimation of the number of N atoms present in a system.

Following from this, a discharge in the laser tube would not be essential for oscillations to occur, rather a flow of some hydrocarbon together with suitably excited nitrogen should, in principle, be sufficient for operation of the laser. An experiment, sketched in Fig.13, was consequently devised along

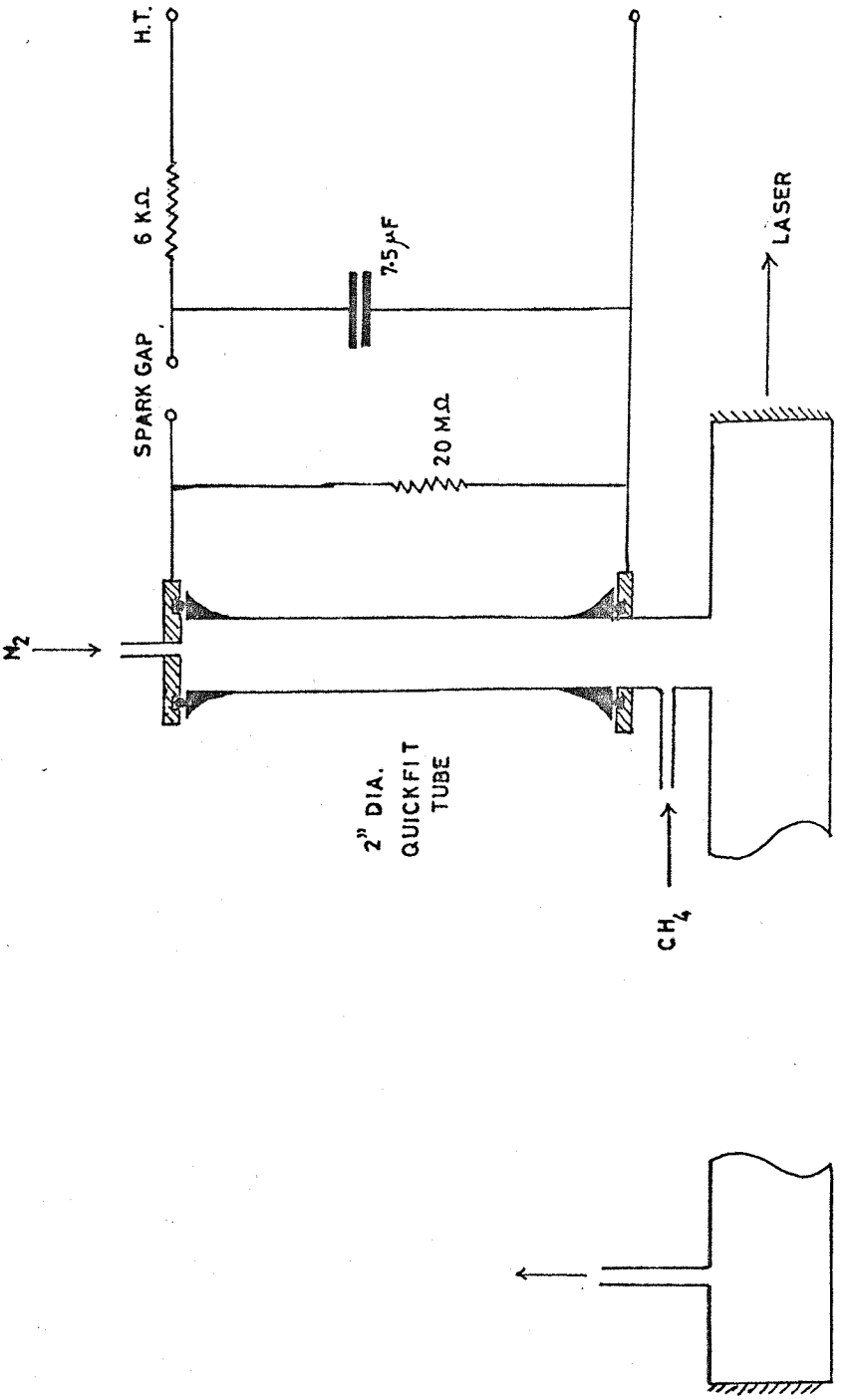

FIG. 13 SIDE ARM EXPERIMENT

these lines. Only nitrogen was excited by a pulsed discharge in a side-arm from the main laser tube. The side arm was a 18" long and 2"i.d. tube with 'Quickfit' ends, with brass electrodes with O-ring seal. Nitrogen was fed through the anode and methane was introduced downstream from the discharge region. The spark gap was simply conttructed from ball-bearings and roughly adjusted to give 10pulses/sec, the choice of this repetition rate was to suit the response time of the Golay cell which was used to detect the output.

Laser oscillations were obtained from this system. The alignment of the cavity was checked by running a CW discharge through the main tube. Imperfections in the spark gap caused the discharge pulses to be very irregular and laser oscillations only occured during some of the pulses. Under the conditions of operation of the laser, the d.c. current flowing into the charging circuit of the spark gap was about 1 amp. at 2.5kV. The pulse length was not measured, but even if it was as long as 100μsec the current in the discharge pulses would have been over 1000A. Because of the irregularity, no quantitative measurements of the laser output could be attempted and hence a more stable means of exciting the nitrogen was aimed for. This is discussed in the next section.

One of the conclusions from the experiment was that the HCN may be formed with an inverted population when nitrogen atoms

react with methane. Alternately, since there is ample evidence in the literature that HCN would be formed in the system, the excitation of HCN could be by some other excited species or by vibrational transfer from excited nitrogen molecules. The latter scheme would seem unlikely considering the energy defect of the levels involved. For the direct excitation of the $11^{1}0$ level of HCN the gap is $470cm^{-1}$ whereas excitation to the 100 level would involve a gap of $230cm^{-1}$ but then excitation of the bending mode would have to be explained. But however the excitation is achieved, the lifetime of the process has to be greater than about 5msec to allow the constituents to travel the 4cm before entering the laser cavity.

4.4 Microwave Excitation of Nitrogen

To overcome the instability problems of a pulsed discharge in nitrogen, microwave excitation of the nitrogen was tried. This is the most common method for dissociating nitrogen for reaction experiments with N atoms. Microwave power at 2.45GHz was obtained from a Mullards JP2-0.2 magnetron. This magnetron is capable of delivering a continuous power of 200 watts, and the circuit of the power supply constructed for it is shown in Fig. 14a and 14b. The timer is provided to allow the heaters to warm for 4 minutes before the H.T. is switched on. Also, the heater voltage has to be reduced by a specified amount when more than 100 watts are being drawn from the magnetron. This was

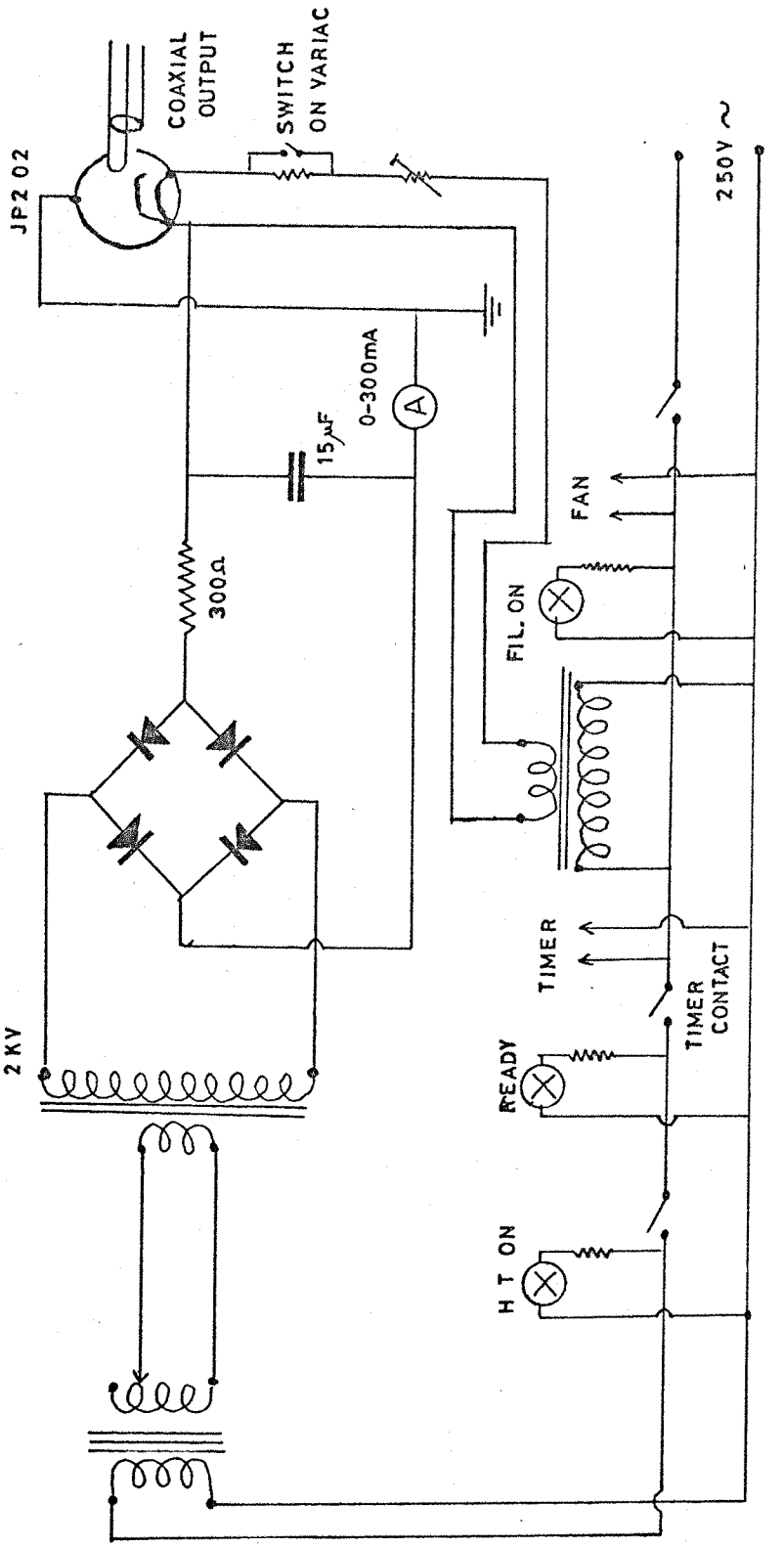

FIG. 14a MAGNETRON POWER SUPPLY

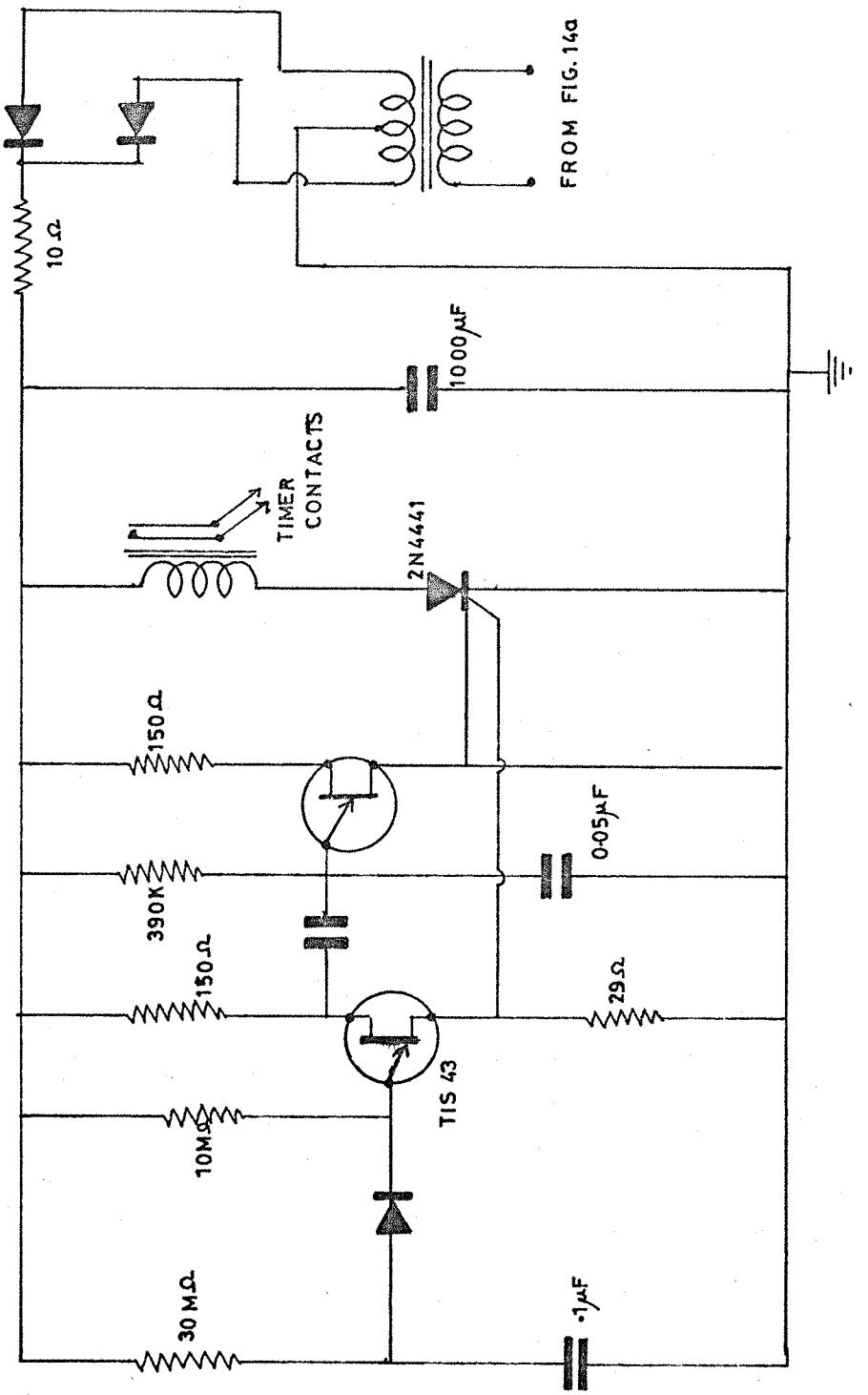

FIG. 14b TIMER FOR MAGNETRON SUPPLY

done by a microswitch, operating on a preset position of the variac, which brought a fractional ohm resistance into the heater circuit. A fixed reflection element was fitted on the output of the magnetron for protection against mismatching of the load. This is essential as sudden mismatches can easily occur if pressure changes in the gas cause the discharge to be extinguished. The reflection element was built from specifications provided by Mullards. Transmission of power to the cavity was by means of a p.t.f.e. insulated co-axial cable, the connections being made by N-type connectors. The microwave cavity, used to couple power to the gas, was of a type which could be slipped onto glass tubes of up to ½" diameter. The amount of power being dissipated required the use of an air compressor to blow air through the cavity for cooling.

In the first experiment tried, nitrogen was excited by the microwave discharge and then mixed with methane before entering the laser cavity. No oscillations could be obtained with this system. The system was then slightly modified to determine whether any gain was produced by the microwave excitation of nitrogen. The set-up used is shown in Fig.15. As before, the microwave excited nitrogen was mixed with methane before entering the cavity and, in addition, the mixture was subjected to a d.c. discharge some 75cm downstream from the point where the gases entered the cavity. The d.c. discharge was used to

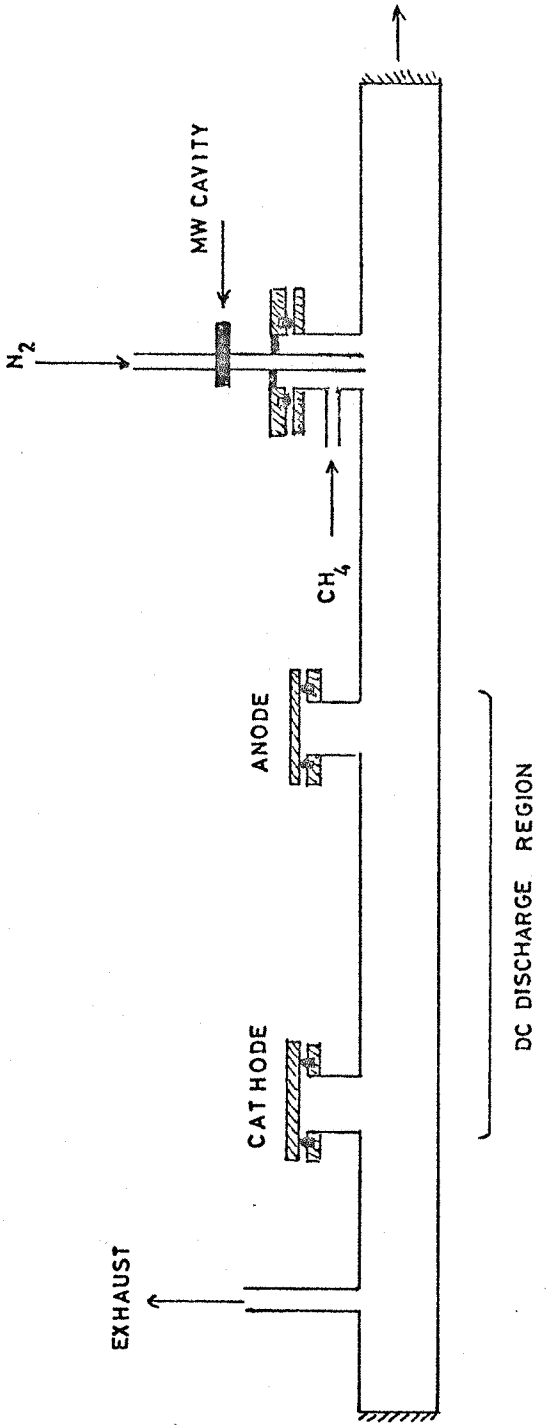

FIG 15 GAIN WITH MW EXCITED NITROGEN

set up the laser oscillating just above threshold. The d.c. current flowing in the discharge at threshold was typically 200mA. The partial pressures of methane and nitrogen were about 0.05 and 0.15torr respectively.

In this configuration, a 50% decrease in the d.c. threshold current could be obtained by putting about 150 watts of microwave power into the nitrogen. Similar results were obtained by mixing excited nitrogen with methyl cyanide or acetone. Acetone worked well with this system, with about 150watts of microwave power, a d.c. discharge of less than 100mA was sufficient to hold the laser in oscillation. The increase in the output power occured after a delay of about a second from the time of switching on the microwave power. This delay presumably corresponds to the time required for the microwave discharge products to reach the region of the d.c. discharge.

Two alternative inferences can be drawn from the observation of gain in this system.

a) N atoms combine with methane to form HCN, but because of the delay in the power increase, the population inversion is in the d.c. discharge. It is known that N atoms combine with most hydrocarbons to produce HCN. Nitrogen molecules in a high vibrational state are believed to contribute to this reaction but the mechanism is not understood.

The observation of laser oscillations in the side-arm experiment described in the previous section could have been

due to the back streaming of the methane molecules into the nitrogen discharge region.

b) The reaction involved is between a long-lived species in active nitrogen (τ = 1sec, to allow it to travel the 75cm distance) and some dissociation product of the hydrocarbon used. This reaction may either produce excited HCN or some other intermediate species which subsequently transfers energy to HCN in a collision.

Rough calculations indicate that if the inversion in the lasing system results from the N atoms reacting with the hydrocarbon to give excited HCN, then oscillations should have been obtained with this system.

The ratio for the reaction of N atoms with methane and ethylene to form HCN are fairly fast - 1.5×10^{-14} and 0.9×10^{-14} $cm^3 molecule^{-1} sec^{-1}$ respectively (Ref. 50 and 51). The recombination rate of N atoms in the presence of molecular nitrogen is extremely slow and is of the order of 5×10^{-33} cm^3 $molecule^{-1} sec^{-1}$. From these rates it is evident that the loss of the N atoms would be primarily due to the reaction with the hydrocarbon, forming HCN as the major product. This has been experimentally verified (Ref.52) when HCN was produced to the extent of 96% of the N atoms destroyed in a reaction with ethylene. The percentage of methane converted to HCN is lower at the temperatures existing in the discharge tube.

An ethylene-active-nitrogen mixture was used to obtain laser oscillations, but contrary to the result which would be expected from the higher percentage formation of HCN, the laser output was approximately 25% lower than that obtained from a methane-active-nitrogen mixture. With a typical operating pressure of 0.1torr and the nitrogen at a flow rate of about 3 litres/sec, the number of nitrogen molecules entering the system would be 10^{19}/sec. If we now make the reasonable assumption of only 1% of the nitrogen molecules being dissociated and 50% of the N atoms combining with ethylene to form HCN in the $1^1\Sigma$ state, then 10^{17} molecules/sec would be produced. This would then roughly correspond to the number of laser photons emitted per second. For the 337μm laser transition this would be equivalent to an output power of about 6×10^{-5}watts. This output power could have been easily detected with the Golay detector used.

The inability of get laser oscillations with this system suggests that although the N atoms could be responsible for the production of HCN, hence accounting for the increase of power observed, some other mechanism inverts the population of the molecule. The possibility of the HCN molecule being formed with an inverted population could still be explained by the reaction of N atoms with some simpler product resulting from the dissociation of the hydrocarbon in the discharge. The methyl radical may thus

be responsible for the lasing mechanism. This possibility seems to be suggested from the lower thresholds obtained with compounds where the methyl radical can be easily separated from the molecule, for example acetone (CH_3-$COCH_3$).

4.5 Experiments with Methyl Radicals

These experiments were devised to determine whether the operation of the laser depended upon the reaction of methyl radicals with N atoms. In order to keep the processes occuring within the laser tube as simple as possible an electrical discharge had to be avoided. Two processes were used for the production of the methyl radicals:

a) Photosensitization of acetone by mercury

b) Thermal decomposition of di-tertiary butyl peroxide.

4.5.1 Photosensitization of acetone

One of the methyl radicals in acetone ($CH_3.COCH_3$) can be easily removed by collision with an excited ($^3P_1$) mercury atom. This process was utilized in designing a system to search for laser oscillations with methyl radicals and active nitrogen. Mercury atoms can be excited very efficiently into the $^3P_1$ state by resonance pumping with mercury vapour lamps. The $^3P_1$ state corresponds to the 2537Å transition to the ground state of the atom.

The layout of the experiment is shown in Fig.16. The centre section of the laser tube was made of quartz so as to transmit the 2537Å radiation from the mercury lamps, which excited the mercury vapour in the laser tube. The four mercury vapour lamps, each 112cm long and emitting about 15watts each at 2537Å were mounted with their axes lying along a cylinder with a radius about 2cm larger than the laser tube. To utilize most of the radiation, a cylindrical reflector lined on the inside with aluminium foil completely enclosed the centre section. The four mercury lamps were connected in series with an 8H choke in the line, and were powered by a 4kV a.c. transformer, the primary of which was controlled by a variac.

The mercury was contained in a vessel which could be heated up to 100°C by water in a surrounding jacket. A thermometer was fitted to measure the temperature. Nitrogen was fed through the vessel containing mercury, to help the flow of the mercury vapour, and this mixture was fed in near to each end of the quartz tube. The quartz tubing between the main tube and the mercury vessel was heated up to about 250°C to prevent condensation of the mercury on the walls. The microwave cavities to excite the nitrogen were situated on this tubing a few cm before the joint on the laser tube.

On either side of the centre quartz section were detachable pyrex sections, in which the electrodes and inlets for acetone were situated. 'Quickfit' ends and clamping flanges were used on all sections to allow rapid dismantling for cleaning.

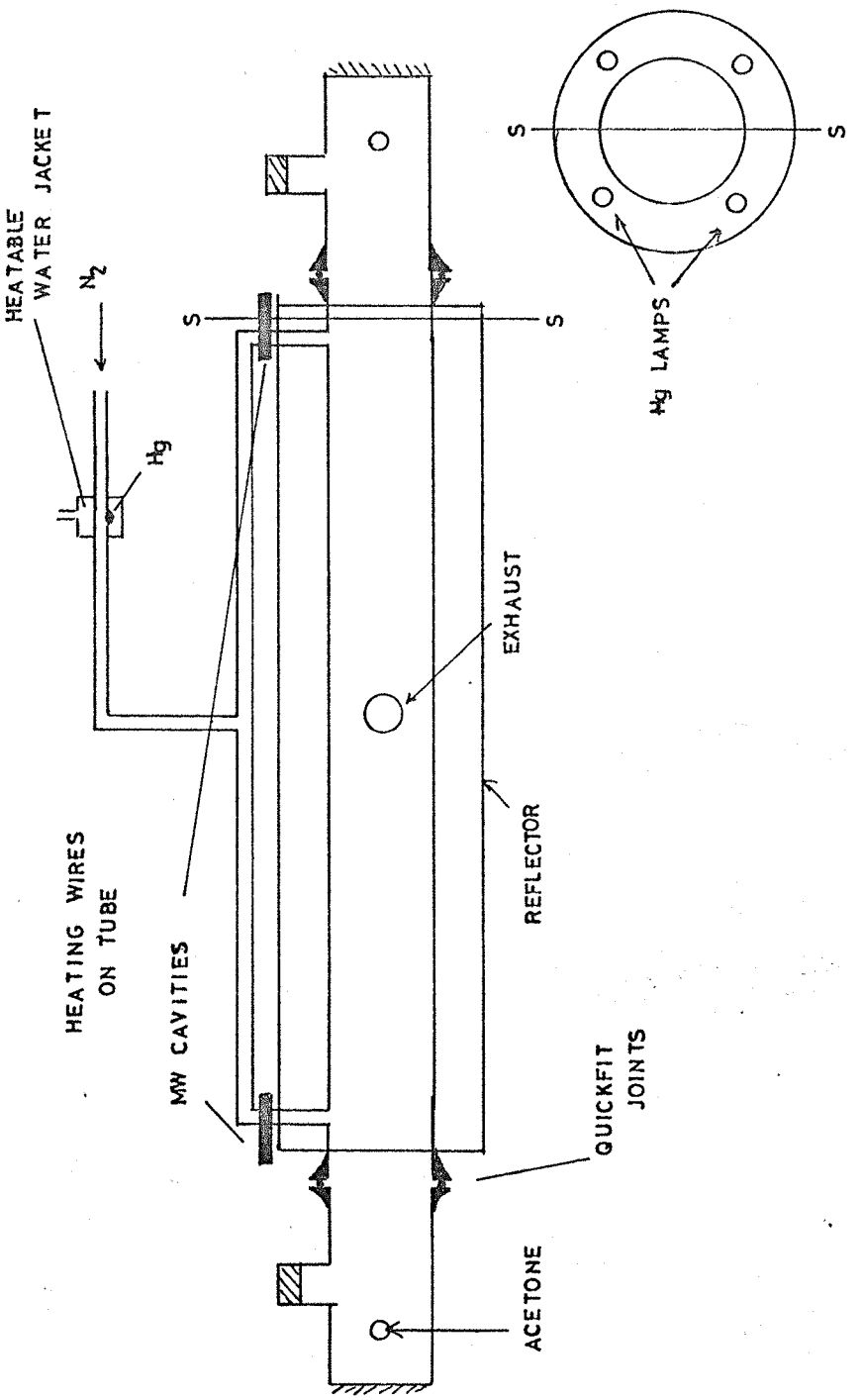

FIG 16 PHOTO-SENSITIZATION OF ACETONE

Fig.17 shows how the absorption of 2537Å radiation from a small mercury lamp was used to estimate the pressure of mercury in the laser tube. The mercury pressure had to be chosen for optimum resonance excitation of the atoms contained in the mode volume of the cavity, i.e. maximum absorption in the region of the tube axis. It can be easily seen that for a narrow beam along the tube diameter the absorption in the mode volume is :

$$I_{abs.} = I_{in} \left[e^{-\alpha(R-r)} - e^{-\alpha(R+r)} \right] \qquad \ldots (4.5.a)$$

where α is the absorption coefficient for 2537Å radiation. By differentiating and equating to zero we get the condition for maximum absorption :

$$\tan \alpha r = \frac{r}{R} \qquad \ldots (4.5.b)$$

$$\text{or} \qquad \alpha \simeq \frac{1}{R} \quad \text{if } \frac{r}{R} \text{ is small} \qquad \ldots (4.5.c)$$

For a laser tube of 5cm diameter, the optimum absorption coefficient is hence $0.4 cm^{-1}$. The absorption coefficient, at the line centre, can be obtained from the expression (Ref.50) :

$$k_o = \frac{2}{\Delta \nu_D} \sqrt{\frac{\ln 2}{\pi}} \quad \frac{\lambda_o^2}{8\pi} \quad \frac{g_2}{g_1} \quad \frac{N}{\tau} \qquad \ldots (4.5.d)$$

$$= \frac{2}{1.1 \times 10^9} \sqrt{\frac{\ln 2}{\pi}} \times \frac{2537^2 \times 10^{-16}}{8\pi} \times 3 \times \frac{N}{1.1 \times 10^{-7}}$$

$$\text{i.e.} \qquad k_o \simeq N \times 6 \times 10^{-13} cm^{-1} \qquad \ldots (4.5.e)$$

where Δ_D is the Doppler broadened linewidth,

λ_o is the wavelength at the line centre,

g_2 and g_1 are the multiplications of the upper and lower level respectively,

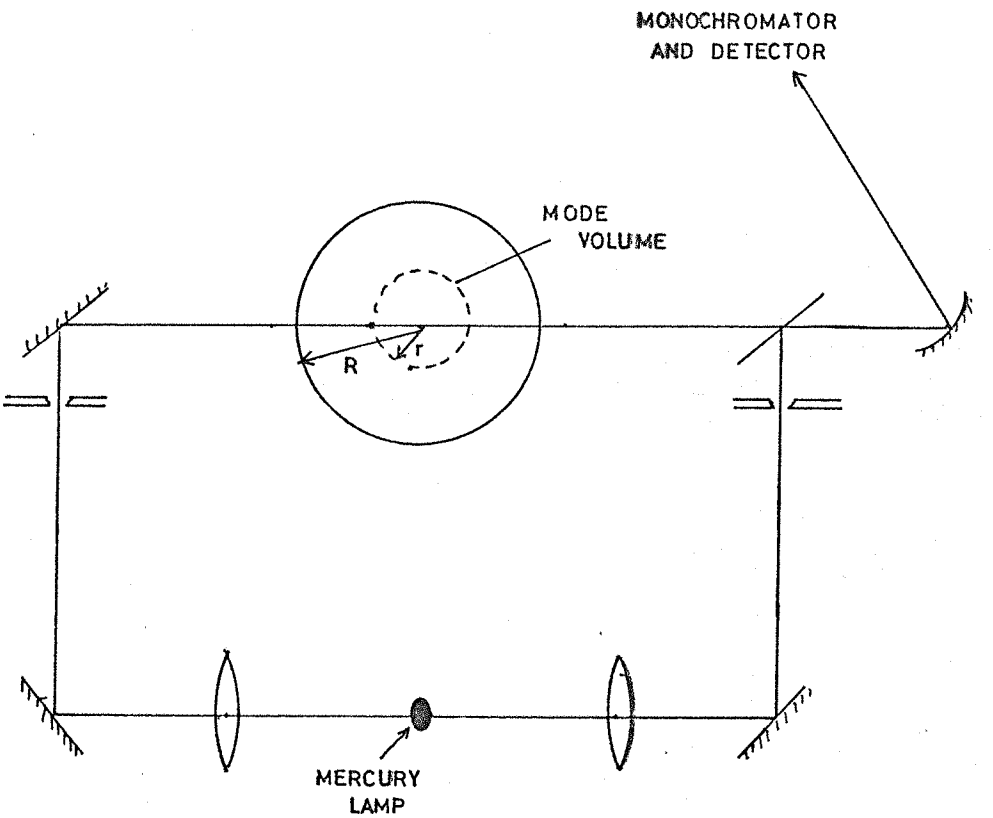

FIG. 17 MONITERING MERCURY ABSORPTION

N is the number of atoms/cc,

and τ is the lifetimes for radiative decay.

The optimum absorption coefficient, $0.4 cm^{-1}$, for this experiment hence corresponds to about 7×10^{11} atoms/cc.

The number of collisions between mercury atoms and acetone molecules is evaluated from kinetic theory :

$$Z = \sigma^2 \left[\frac{8\pi RT(M_{Hg}+M_{Ac})}{M_{Hg}M_{Ac}}\right]^{\frac{1}{2}} \times N_{Hg} \times N_{Ac} \qquad \ldots (4.5.f)$$

or

$$Z \simeq 3.6 \times 10^{-10} \times N_{Hg} \times N_{Ac} \ cm^{-3} sec^{-1} \qquad \ldots (4.5.g)$$

where $\sigma^2 = 32 \times 10^{-16} cm^2$ (Ref.51) is the collision cross-section for mercury atoms with acetone molecules,

R = the gas constant in ergs/deg/mole,

M_{Hg}, M_{Ac} are the molecular weights, respectively of the mercury atoms and acetone molecules,

and N_{Hg}, N_{Ac} are the concentrations of the mercury atoms and acetone molecules respectively in molecules/cc.

The requirement of maximum absorption in the region of the tube axis fixes the pressure of mercury. There is also a limitation on the acetone pressure because, for an efficient system, the radiative lifetime of an excited mercury atoms must be large compared to the lifetime for collisional deactivation by acetone molecules. With the value for the concentration of mercury atoms equation (4.5.g) becomes:

$$Z \simeq 250 \times N_{Ac} \ cm^{-3} sec^{-1} \qquad \ldots (4.5.h)$$

The lifetime of an excited $^3P_1$ mercury atom, for radiative decay τ_{rad}, is 1.1×10^{-7} sec (Ref.50) and, in the configuration used here, for deactivation by an acetone molecule is :

$$\tau_c = \frac{N_{Hg}}{Z} \simeq \frac{7 \times 10^{11}}{250 \times N_{Ac}}$$

For τ_{rad} to be larger then τ_c :

$$1.1 \times 10^{-7} > \frac{7 \times 10^{11}}{250 \times N_{Ac}}$$

or $$N_{Ac} > 2.5 \times 10^{16} \text{ molecules/cc.}$$

Hence, for an acetone pressure of 0.5torr (1.8×10^{16} molecules/cc), which is typically optimum for d.c. laser operation, the probabilities for deactivation by acetone and for radiative decay are nearly of the same order.

We now assume that only the processes occuring within a 2cm diameter cylinder, co-axial with the tube, can contribute to the laser action. From eqn. (4.5.a), with a value of $0.4 cm^{-1}$ for α, about 30% of the intensity incident on the tube would be absorbed in the 2cm diameter cylinder. The maximum power available at 2537Å is 60watts over a 1 metre length. Hence, also allowing for a 50% loss in the reflector, 10 watts are coupled in. If 0.5torr acetone pressure is used, 50% of the power is lost by the radiative decay of the mercury atoms and about 5 watts are available for decomposing acetone molecules to form methyl radicals. Considering the idealized condition, every methyl radical formed would be converted (by reaction with N and N^*_2) into excited HCN

which then decays by emitting a laser photon. The laser output power would then simply be the absorbed energy divided by the ratio of the energies of the 2537Å and 337μm photons, i.e. an output of about 4mW. This output could be possibly doubled if a high enough acetone pressure was used, the radiation of the mercury atoms in this condition being negligible compared to the deactivation by acetone. This laser output is large compared to that obtained with a d.c. discharge in the same length. A considerably lower efficiency, in the production of excited HCN molecules in the $11^{1}0$ state from methyl radicals, would still give a significant laser output.

The calculations above have been made with the approximation that the flow rate is infinitely fast so that the change in concentration of acetone, due to its decomposition, is negligible. With fast adsorption pumps it is possible to approach this condition, but with the 3 litres/sec pumping speed used in our system this factor should be taken into account for a more exact description of the processes. The calculations are hence only used as a guide and they clearly show that, if this mechanism is operative, laser action should be obtained.

Laser oscillations could not be obtained with this system. Also no information could be obtained regarding the existence of any gain in the cavity. The method described before was used to search for gain, but a few minutes of operation of the laser with

a low current d.c. discharge, deposited enough polymer on the walls of the discharge tube to render it opaque to the 2537Å pumping radiation. During the experiment the mercury lamps produced ozone in large quantities and the air in the laboratory was found to contain more than the toxic concentration. This was overcome by extracting the air from the jacket enclosing the lamps and venting it outside the laboratory.

4.5.2 Thermal decomposition of peroxide

The thermal decomposition of di-tertiary butyl peroxide is frequently used as a source of methyl radicals. Only a moderate temperature of 150-200°C is required to break the bond between the oxygen atoms in the peroxide forming a complex which subsequently breaks up into acetone and a methyl radical :

$$(CH_3)_3CO\text{-}OC(CH_3)_3 \longrightarrow 2(CH_3)_3CO$$

$$(CH_3)_3CO \longrightarrow (CH_3)_2CO + CH_3$$

The equipment used for the experiment was essentially the same as that for the photo-sensitization of acetone (see Fig.16). The mercury lamps and reflector were removed and heating wire was wound on asbestos round the quartz centre section of the laser tube. The tube could be heated up to 300°C using the mains supply controlled by a variac. A thermocouple on the tube monitored the temperature.

No laser oscillations could be obtained. However, when the laser was operated with the d.c. discharge, microwave excitation

of the nitrogen coupled with the thermal dissociation of the peroxide was effective in lowering the threshold from about 100mA to only 10mA. On one occasion the laser operated on only 4mA d.c. current through the tube, but subsequently this could not be repeated.

The thick brown polymer which deposits on the walls of the tube has a significant effect on the operation of the laser under the conditions used in the experiment. With a clean tube the threshold is comparatively high, but with continued operation the threshold slowly decreases to a minimum value after which the threshold rises again. After a few days of operation the tube cannot be made to oscillate. The behaviour of the laser was hence not repeatable from day to day. However, the consistent result when operating with the peroxide is that the threshold of the laser can be decreased, by almost an order of magnitude, when the tube is heated and a microwave discharge applied to the nitrogen entering the cavity.

The presence of the d.c. discharge would result in the creation of a number of species whose identity cannot be easily determined and this complicates the interpretation of the experiment. The following inferences can be drawn from the results of the methyl radical experiments:

a) It seems unlikely that methyl radicals combining with N atoms are directly responsible for the laser action.

b) The low threshold observed with the peroxide could be due to the higher efficiency of N atoms combining with methyl radicals to produce HCN compared with that of the hydrocarbons normally used. The percentage production of HCN when N atoms combine with methyl radicals is not known. With this mechanism some other process would be required for the excitation of the HCN produced.

c) The bending mode ν_2 of the HCN molecule corresponds to $712cm^{-1}$, and at a gas temperature of $300^{o}C$ roughly 17% of the molecules could be expected to be in the $01^{1}0$ state. A subsequent vibrational transfer of energy, equivalent to the ν_1 mode, could then be responsible for the excitation to the $11^{1}0$ state. The energy may be transferred from vibrationally excited nitrogen molecules, but the $240cm^{-1}$ energy defect for the process suggests that some other species could have a greater probability for exciting the HCN molecule. The polymer formation on the walls indicates the presence of long-chained complexes and one of the numerous intermediate species, if produced in sufficient numbers, could be more likely in effecting the vibrational transfer.

4.6 Experiments with HCN

In order to try to separate the processes involved in the production of HCN from the processes which produce the inversion, it was decided to use pure HCN. There is no report in the literature of continuous operation of the laser using pure HCN.

The HCN was obtained in liquid form in a 2lb steel cylinder from I.C.I. As HCN is very poisonous, the handling procedure was carefully worked out and followed in detail. The operator wore a 'Puretha' type gas mask whenever liquid HCN was handled. In addition, one of the policies was to always have a second person present besides the operator. Handling procedure, safety precautions, preparation of test solutions, and other relevant details are described in the literature supplied by I.C.I.

A few millimetres of liquid HCN was transferred from its cylinder to a small stainless-steel container. A needle valve on top of this container could be directly attached to the gas handling system of the expermment. The liquid was transferred by a suction pipette in a poisons fume cupboard, and, to safeguard aginst possible leaks in the container, an outer container was used for transporting to the laboratory (see Fig.18).

The entire laser system was enclosed by sheet polythene supported by a 9'x3'x3' frame. An exhaust fan backed by a vacuum cleaner motor drew air from the enclosure and bubbled it through an alkaline solution to precipitate and detoxify any leaks of HCN.

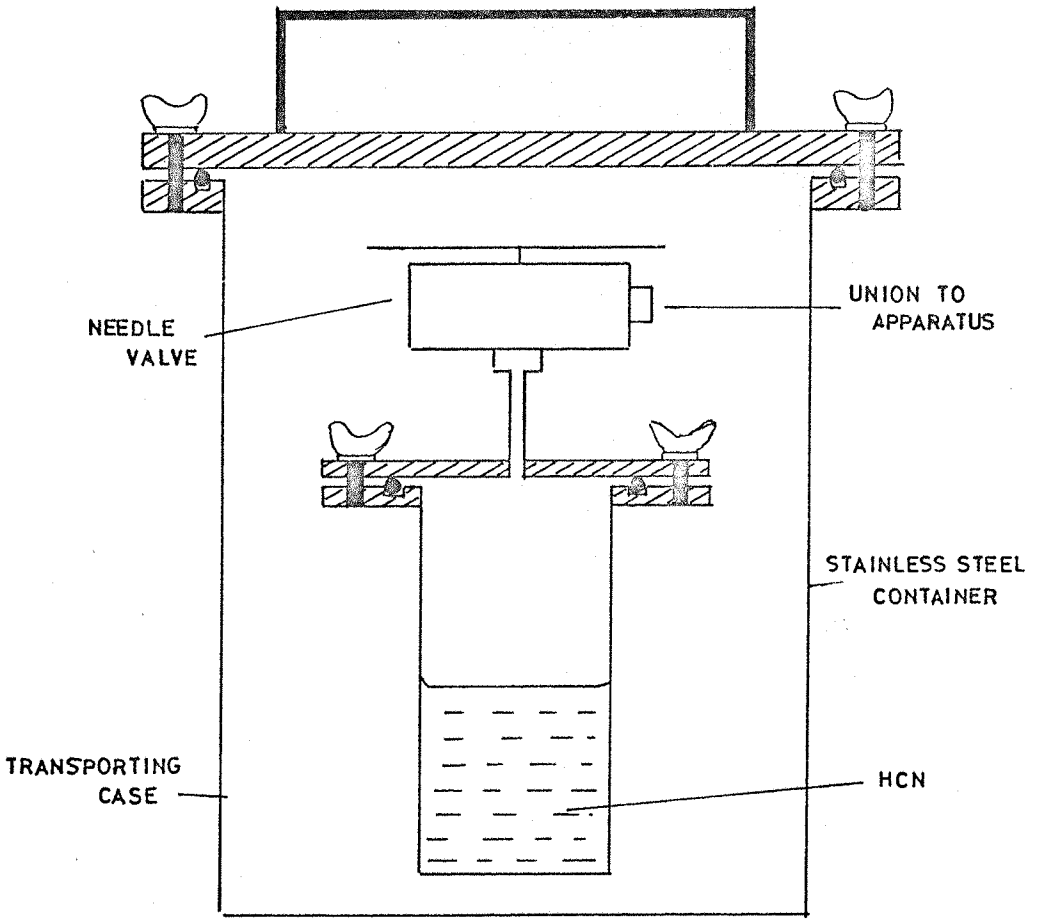

FIG 18 HCN CONTAINER

The system was tested by removing the top cover of the HCN container within the polythene enclosure. Although a positive indication was obtained near an opening close to where the HCN container is located, the concentration of HCN in the laboratory was well below the toxic limit.

With about 0.2torr HCN flowing through the tube, the laser operated with a d.c. current threshold of about 150mA. This threshold is higher than that observed with either acetone or peroxide. Addition of nitrogen decreased the threhsold and 'active' nitrogen further lowered the threshold down to about 50mA. This is again much higher than the typical 10mA achievable with the peroxide. Carbon monoxide had roughly the same effect on the laser output as nitrogen. Carbon monoxide was used because the energy defect of vibrational transfer to the $_1$ normal mode of HCN is only $68cm^{-1}$ as compared to the $240cm^{-1}$ of nitrogen.

Following one of the inferences from the previous section, the laser tube was heated to $300^{o}C$, with HCN flowing through the tube, to get some population in the $01^{1}0$ state. Either carbon monoxide or nitrogen was then admitted into the tube, after excitation by a microwave discharge, in an attempt to pump HCN from the $01^{1}0$ state into the $11^{1}0$ state. Heating the tube decreased the laser output power by roughly 25% and the addition of excited carbon monoxide or nitrogen did not have a significant effect on the laser output. The lower laser level in many systems

is generally depleted by collisions with the 'cold' walls of the tube. Heating the tube could significantly lower this relaxation rate and the experiment described may not have worked for this reason alone. However, the population rates from nitrogen and carbon monoxide would be expected to have a significant difference because of the different gaps for energy transfer. The failure to observe the resulting difference in laser output seems to rule out this simple vibrational transfer scheme.

Swwithing on a d.c. discharge of about 0.4amps through HCN causes dissociation and subsequent polymer formation to such an extent that the pressure, monitored at the outlet of the tube, drops by a factor of about 2. Compared with a methane-nitrogen mixture this polymer formation is very rapid. A few hours of operation at currents lower than 200mA completely clogs the tube and extinguishes laser action. A 1-amp current through a mixture of about 0.2torr water vapour and 0.2torr nitrogen have been found to be very effective in cleaning the tube. One disadvantage is that operation with this mixture seems to attack the O-rings which are used to seal the electrodes to the laser tube.

From an operational point of view, running on pure HCN does not seem to have any advantage over other compounds and mixtures. Among the disadvantages are the hazards associated with handling pure HCN, excessive polymer deposition and lower laser output power.

4.7 Conclusions

The theory of Lide and Maki (ref.28) explaining the laser in terms of the HCN molecule seems to be valid. The series of experiments reported here lead to some information regarding the processes occuring within the discharge tube.

To a first approximation the laser output does not depend on the active material as long as the three elements H, C and N are present. Summarising the information obtained from the experiments performed :

1. Active nitrogen reduces the threshold for oscillation in all mixtures tried. The effect is most pronounced in the peroxide-nitrogen mixture where the threshold drops to 10mA.
2. Behaviour of pure HCN in a d.c. discharge is similar to that of peroxide-nitrogen.
3. There is a $\sim$30% increase in output when HCN is introduced to a peroxide-nitrogen discharge.
4. Output from a d.c. discharge in HCN improved by adding N_2. Further improvement by the microwave excitation of nitrogen.
5. Carbon monoxide has an effect similar to nitrogen on the output from HCN.
6. Striking a discharge in pure HCN reduces the pressure by a factor of $\sim$2.
7. The increase in output by adding excited CO to methyl cyanide is an order of magnitude greater than that obtained by adding excited nitrogen.

8. Failure to obtain an enhancement in the output power when the laser tube was heated to 300°C with flowing HCN, to provide population in the $01^{1}0$ state.

From these points we can draw some conclusions regarding the inversion mechanism of the HCN laser. Considering first the possibility of electronic excitation there could be two mechanisms:

a) Excitation to an electronic state and subsequent decay to the ground state with an inverted population.

b) Direct excitation of the vibrational levels in the ground state.

Even if the levels of interest ($11^{1}0$ and $04^{0}0$) were excited with the same rates by either process a or b, a population inversion could still be achieved if the relative decay rates are favourable. However, though this may give a small contribution, it does not seem to be the dominant mechanism. This follows from the observation that pure HCN does not give a higher output than a typical organic mixture. Also, adding HCN to various mixtures does not significantly increase the output and it would not be obvious why exciting nitrogen results in such a large increase in output.

The possibility of direct vibrational transfer from $N_2(v=1)$ to the HCN molecule can be easily eliminated because a HCN-N_2 mixture would be expected to give considerably higher power than those obtained from various organic mixtures. Also heating the laser tube to 300°C, with flowing HCN, would be expected to

significantly populate the $01^{1}0$ level and hence the vibrational transfer from either N_2 v=1 or CO v=1 would have a larger probability. This was not observed.

The remaining possibility is that of inversion resulting from chemical reactions within the discharge tube. The possible processes are :

a) Chemical formation of HCN with an inverted population.

b) Production of HCN in the ground state together with the formation of some excited species which inverts the HCN population by vibrational transfer.

There are many observations to support process a, for example compounds with lower dissociation energies have lower threshold for oscillation and hence explains the extremely low threshold obtained with the peroxide. Active nitrogen is known to convert hydrocarbons very efficiently into HCN and, as observed, this would result in higher output. However, the addition of HCN to a peroxide-nitrogen mixture gives roughly a 30% increase in output and, taking the relative dissociation energies into account, this behaviour cannot be explained.

The process b is hence suggested as the inversion mechanism as every single observation can be explained in terms of it. Recent articles in the literature (Ref. 44 and 45) suggest that the energy defect between the levels for vibrational transfer can be much larger than that calculated with existing theories. This

would make it relatively simple for an excited intermediate species, formed by the recombination of various radicals and molecules present in the discharge, to transfer vibrational energy to the HCN molecule. Also considering the ease with which this laser operates with different mixtures, giving roughly similar outputs, the structure of the intermediate species responsible may not be the same for the different mixtures.

REFERENCES

1. L.E.S. Mathias and J.T. Parker, 'Stimulated emission in the band spectrum of N_2', Appl. Phys. Lett., 3, 16 (1963).

2. L.E.S. Mathias and J.T. Parker, 'Visible laser oscillations from CO', Phys. Lett., 7, 194 (1963).

3. A. Crocker et al., 'Stimulated emission in the far infra-red', Nature, 201, 250 (1964).

4. H. Steffen et al., 'Comments on a new laser emission at 0.774mm wavelength from ICN', Phys. Lett., 21, 425 (1966).

5. H.A. Gebbie et al., 'A stimulated emission source at 0.34mm wavelength', Nature, 202, 685 (1964).

6. L.E.S. Mathias et al., 'Laser oscillations at sub-millimetre wavelengths from compounds of H, C and N', Electronics Lett., 1, 45 (1965).

7. W.M. Muller and G.T. Flescher, 'CW submillimetre oscillations in H_2O, D_2O and CH_3CN', Appl. Phys. Lett., 8, 217 (1966).

8. H. Steffen et al., 'Stimulated emission up to 0.538mm wavelength from cyanic compounds', Phys. Lett., 20, 20 (1966).

9. S. Kon et al., 'Experiments on a far infra-red CN laser', Jap. Jour. Appl Phys., 6, 612 (1967).

10. W.M. Muller and G.T. Flescher, 'CW submillimetre oscillations in discharges containing C, N and H or D', Appl. Phys. Lett., 10, 93 (1967).

11. O.M. Stafsudd et al., 'Laser action in selected compounds containing C, N and H or D', IEEE Jour. Q.E., QE-3, 618 (1967).

12. H. Yoshinaga et al., 'Far infra-red gas lasers', Science of Light, 16, 50 (1967).

13. L.E.S. Mathias et al., 'Spectroscopic measurements on the laser emission from discharges in compounds of H, C and N', IEEE Jour. Q.E., QE-4, 205 (1968).

14. V.J. Corcoran et al., 'CW gain characteristics of the 890-GHz HCN laser line', IEEE Jour. Q.E., QE-5, 292 (1969).

15. O.M. Stafsudd and Y.C. Yeh, 'The CW gain characteristic of several gas mixtures at 337μm', IEEE Jour. Q.E., QE-5, 377 (1969).

16. J.P. Kotthaus, 'High power output from a submillimetre CW gas laser Appl. Opt., 7, 2422 (1968).

17. V. Sochor and E. Brannan, 'Time dependence of the power output at 337μm in a CN laser', Appl. Phys. Lett., 10, 232 (1967).

18. M. Yamanaka et al., 'Time dependence of pulsed output, transverse mode pattern and polarization characteristics in far infra-red CN lasers', Jap. Jour. Appl. Phys., 7, 250 (1968).

19. R. Turner et al., 'Multiple pulse emission from a HCN laser', Appl. Phys. Lett., 12, 104 (1968).

20. R.G. Jones et al., 'Transient phenomena in the 337μm maser', Appl. Opt., 8, 701 (1969).

21. L.O. Hocker et al., 'Absolute frequency measurement and spectroscopy of gas laser transitions in the far infra-red', Appl Phys. Lett., 10, 147 (1967).

22. L. O. Hocker and A. Javan, 'Absolute frequency measurement on new CW HCN sub-millimetre laser lines', Phys. Lett., 25A, 489 (1967).

23. P.G. Frayne, 'Repetitive Q-modulated HCN gas maser', Jour. Phys. B., 2, 247 (1969).

24. R. Turner and T.O. Poehler, ' Emission from HCN and H_2O lasers in the 4 to 13μm region', Phys. Lett., 27A, 479 (1968).

25. G.W. Chantry et al., 'A suggested mechanism for the 337μm CN maser', Nature, 205, 377 (1965).

26. H.P. Broida et al., 'Comments on the mechanism of the 337μm CN laser ', Jour. Appl. Phys., 36, 3355 (1965).

27. H. Steffen et al., 'Mechanism of the sub-millimetre laser emissions from the CN-radical', Phys. Lett., 23, 313 (1966).

28. D.R. Lide and A.G. Maki, 'On the explanation of the so-called CN laser', Appl. Phys. Lett., 11, 62 (1967).

29. T. Li, 'Losses and modes in maser resonators with circular mirrors', Bell Sys. Tech. Jour., 44, 917 (1965).

30. D.E. McCumber, 'Eigenmodes of a symmetric cylindrical confocal laser resonator and their perturbation by output coupling apertures', Bell. Sys. Tech. Jour., 44, 333 (1965).

31. C.K.N. Patel et al., 'High gain gaseous optical masers', Appl. Phys. Lett., 1, 84 (1962).

32. G.D. Boyd and J.P. Gordon, 'Confocal multimode resonator for millimetre through optical wavelength masers', Bell Sys. Tech. Jour., 40, 489 (1961).

33. H. Steffen et al., 'Resonator modes and splitting of the 0.337mm emission of the CN laser', Jour. Appl. Phys., 38, 3410 (1967).

34. A. Camani et al., 'Cyan-Verbindungen in Sub-millimeterwellen-Gaslaser', Z. Angew. Math. Phys., 16, 562 (1965).

35. A.G. Maki, 'Assignment of some DCN and HCN laser lines ', Appl. Phys. Lett., 12, 122 (1968).

36. G. Amat and H. Nielsen, 'Rotational distortion in linear molecules arising from ℓ-type resonance', Jour. Mol. Spec., 2, 163 (1958).

37. A.G. Maki and D.R. Lide, 'Microwave and infra-red measurements on HCN and DCN', Jour. Chem. Phys., 47, 3206 (1967).

38. D.H. Rank et al., 'Vibration-rotation spectra of HCN', Jour. Opt. Soc. Am., 50, 421 (1960).

39. A.G. Maki and L.R. Blaine, 'Infra-red spectra of HCN from 2000 to 3600cm^{-1}', Jour. Mol. Spec., 12, 45 (1964).

40. W.W. Brim, 'Measurements on higher J rotational lines of vibration-rotation bands and study of resonances in linear polyatomic molecules', Jour. Opt. Soc. Am., 50, 1208 (1960).

41. A.L. Waksberg and A.I. Carswell, 'Optical resonator effects on the population distribution in He-Ne gas lasers determined from side-light measurements', Appl. Phys. Lett., 6, 137 (1965).

42. M. Anson and A.A. de Soyza, 'A low noise amplifier for indium antimonide infra-red detectors', Jour. Sci. Inst., 1, 952 (1968).

43. A.N. Wright and C.A. Winkler, 'Active Nitrogen', Academic Press, 1968.

44. R.W.F. Gross, 'Chemically pumped CO_2 laser', Jour. Chem. Phys., 50, 1889 (1969).

45. T.A. Cool et al., 'DF-CO_2 and HF-CO_2 continuous wave chemical lasers', Appl. Phys. Lett., 15, 318 (1969).

46. H. Steffen and F.K. Kneubuhl, 'Resonator interferometry of pulsed sub-millimetre wave lasers', IEEE Jour. Q.E., QE-4, 992 (1968).

47. A.L. Schawlow, 'Investigation of coherent sources of infra-red radiation', U.S. Govt. Report N69-12011, Clearinghouse, (August 1968)

48. H. Steffen et al., 'Relations between modes and pulse shapes of submillimetre wave laser emission', Electronic Lett., 3, 561 (1967)

49. G.E. Hyde and D.F. Hornig, 'The measurement of bond moments and derivatives in HCN and DCN from infra-red intensities', Jour. Chem. Phys., 20, 647 (1952).

50. A.C.G. Mitchell and M.W. Zemansky, 'Resonance radiation and excited atoms', Cambridge University Press (1961).

51. B. deB. Darwent et al., 'Quenching of mercury resonance radiation', Jour. Chem. Phys., 22, 859 (1954).

52. S. Kon et al., 'Spatially resolved measurement of plasma density using a 337μm cyanide laser', Jap. Jour. Appl. Phys., 7, 434 (1968).

53. V.J. Corcoran et al., 'Frequency lock of ths hydrogen cyanide laser to a microwave frequency standard', IEEE Jour. Q.E., QE-5, 424 (1969).

54. C.G.B. Garrett, 'Far infra-red masers and their applications to spectroscopy', Physics of Quantum Electronics.

55. G.C. Thomas, 'Proposal for a new determination of the velocity of light', Seminar, Dept. of Electronics, Southampton University (August 1968).

56. V. Daneu et al., 'Accurate laser wavelength measurements in the infra-red and far infra-red using a Michelson interferometer', Phys. Lett., 29A, 319 (1969)

57. J.M. McMahon, 'Laser mode selection with slowly opened Q-switches', IEEE Jour. Q.E., QE-5, 489 (1969)

58. D.H. Arnold and D.C. Hanna, 'Transverse mode selection of rotating mirror Q-switched lasers', Electronics Lett., 5, 16, (1969).

ACKNOWLEDGEMENTS

The author would like to thank all the members of staff and research students of the Laser Group for the innumerable discussions and advice during the project.

For his interest, help and encouragement, the author is especially indebted to the project supervisor, Dr. G.C. Thomas.